AAEC/E450

AAEC/E450

2

AUSTRALIAN ATOMIC ENERGY COMMISSION

RESEARCH ESTABLISHMENT

LUCAS HEIGHTS

A REACTOR PHYSICS SURVEY OF WATER MODERATED, URANIUM-ALUMINIUM PLATE FUELLED RESEARCH REACTORS FOR A RANGE OF URANIUM ENRICHMENT

by

G.S. ROBINSON

July 1979

ISBN 0 642 59673 5

AUSTRALIAN ATOMIC ENERGY COMMISSION
RESEARCH ESTABLISHMENT
LUCAS HEIGHTS

A REACTOR PHYSICS SURVEY OF WATER MODERATED, URANIUM-ALUMINIUM PLATE FUELLED RESEARCH REACTORS FOR A RANGE OF URANIUM ENRICHMENT

by

G.S. ROBINSON

ABSTRACT

The results obtained from reactor physics calculations of water moderated research reactors with fuel in the form of uranium-aluminium alloy plates are presented. The major parameters considered are uranium enrichment, uranium weight per cent in the fuel meat, ^{235}U loading per plate and the water gap between plates. The calculations are based on the SILOE reactor and particular emphasis is placed on the requirements for a proposed new AAEC research reactor. Sufficient detail is given to enable the determination of core size, fuel consumption rate and neutron flux levels in the core and reflector when this study is combined with a thermal-hydraulic analysis.

National Library of Australia card number and ISBN 0 642 59673 5

The following descriptors have been selected from the INIS Thesaurus to describe the subject content of this report for information retrieval purposes. For further details please refer to IAEA-INIS-12 (INIS: Manual for Indexing) and IAEA-INIS-13 (INIS: Thesaurus) published in Vienna by the International Atomic Energy Agency.

ENRICHED URANIUM; FUEL PLATES; ALUMINIUM ALLOYS; REACTOR KINETICS; WATER MODERATED REACTORS; RESEARCH REACTORS; AAEC; REACTOR CORES; ALLOY NUCLEAR FUELS

CONTENTS

		Page
1.	INTRODUCTION	1
2.	FOUR-PARAMETER SURVEY CALCULATIONS	2
	2.1 Parameters	2
	2.2 Power Normalisation	3
	2.3 Major Assumptions	3
	2.4 General Description of Calculation Method	5
	2.5 Molybdenum Activity	6
	2.6 Description of Tabulated and Graphical Results	6
3.	ADDITIONAL INVESTIGATIONS	10
	3.1 General	10
	3.2 RZ Calculations of Various D_2O Reflectors	10
	3.3 RZ Calculations of Various Be Reflectors	11
	3.4 XY Calculations	11
	3.5 Core Size Effect	13
	3.6 Burnup Effect	13
	3.7 Volume Fraction Assumptions	14
	3.8 Axial Reflector	14
	3.9 Sample Worth	15
	3.10 Fuel Element Smearing	15
	3.11 Thermal Poison Worth	15
	3.12 Xenon Override	15
	3.13 Beam Tube Worth	16
4.	CONCLUSIONS	16
5.	REFERENCES	18

Table 1	Case Description	19
Table 2(a)	Reactivity for 2.1 mm Water Gap	20
Table 2(b)	Reactivity for 1.6 mm Water Gap	21
Table 2(c)	Reactivity for 2.6 mm Water Gap	22
Table 3(a)	Form Factors and Core Thermal Flux for 2.1 mm Water Gap	23
Table 3(b)	Form Factors and Core Thermal Flux for 1.6 mm Water Gap	24
Table 3(c)	Form Factors and Core Thermal Flux for 2.6 mm Water Gap	25
Table 4(a)	Fast and Epithermal Flux for 2.1 mm Water Gap	26

(Continued)

CONTENTS (Continued)

		Page
Table 4(b)	Fast and Epithermal Flux for 1.6 mm Water Gap	27
Table 4(c)	Fast and Epithermal Flux for 2.6 mm Water Gap	28
Table 5(a)	Molybdenum Activity and Reflector Flux for 2.1 mm Water Gap	29
Table 5(b)	Molybdenum Activity and Reflector Flux for 1.6 mm Water Gap	30
Table 5(c)	Molybdenum Activity and Reflector Flux for 2.6 mm Water Gap	31
Table 6	RZ Calculations with Various D_2O Reflectors	32
Table 7	RZ Calculations with Various Be Reflectors	33
Table 8	XY Calculations	34
Table 9	Core Size Effect	35
Table 10	Miscellaneous Effects	36
Table 11	Fuel Cycle Information and Molybdenum Activity at 35 MW	37
Table 12	Fuel Cycle Information and Molybdenum Activity for Minimum Fuel Consumption	38

Figure 1	RZ geometry layout	39
Figure 2	XY rectangular layout	40
Figure 3	14.72 g per plate molybdenum activity and reactivity	41
Figure 4	10 g per plate molybdenum activity and reactivity	42
Figure 5	7.36 g per plate molybdenum activity and reactivity	43
Figure 6	2.1 mm water gap molybdenum activity and reactivity	44
Figure 7	Fuel consumption rate	45
Figure 8	Supercell Model	46

Appendix A	Details of the Calculations	47

1. INTRODUCTION

As a consequence of the proposed US policy of restricting uranium enrichment to 20 per cent, the studies for a possible new AAEC research reactor for which fully enriched fuel was initially envisaged have been extended to cover a range of enrichment. This study is concerned with reactor physics aspects of water moderated systems employing fuel plates with a meat of uranium-aluminium alloy. The results of calculations presented here need to be combined with those of a thermal-hydraulic analysis to assess the performance of the systems studied. These calculations have been performed in more detail than is appropriate to a general survey, to enable the following to be determined:

(i) the extent to which the requirements for the proposed new reactor can be met with various enrichments, and

(ii) the core size, power level and fuel consumption rate necessary to best meet those requirements and hence the relative costs associated with various fuel enrichments.

The two major requirements for the new reactor may be summarised as:

(i) a high specific activity for ^{98}Mo irradiation (6 Ci* g^{-1} of natural molybdenum), and

(ii) a high thermal flux ($\sim 5 \times 10^{14}$ neutrons cm^{-2} s^{-1}) over a large reflector volume for the extraction of a number of neutron beams.

The additional requirements for fast neutron flux in the core for materials testing, and for thermal flux in the reflector for isotope production are not as demanding.

To make this survey more realistic, the calculations were based on the fuel element of an existing reactor, namely, the French SILOE reactor. Details of the 15 MW SILOE are included in the IAEA reactor directory [1964] and information on uprating to 35 MW has been given by Merchie [1971]. The parameters used in the survey were, thus, variations on the parameters of a SILOE fuel element. The calculations performed may be divided into two sections: in the first, a four-parameter survey was made under a number of assumptions; in the second, the effect of the more important of these assumptions was investigated and some additional information calculated for particular systems. The four parameters considered were:

(a) uranium enrichment,

---

* 6 Ci $\approx 2 \times 10^{11}$ Bq

(b) uranium weight per cent in the fuel meat,

(c) ^{235}U loading per fuel plate, and

(d) water gap between fuel plates.

To permit the results of this survey to be compared with similar surveys performed elsewhere, the results of calculations are presented in some detail. In addition, a detailed description of the calculations performed is included in Appendix A.

2. FOUR-PARAMETER SURVEY CALCULATIONS

2.1 Parameters

In performing this survey, the parameters chosen were varied about the values for a SILOE fuel plate. A SILOE fuel plate of 26 wt % uranium-aluminium alloy contains 14.72 g of ^{235}U as 93 per cent enriched uranium and has meat dimensions of 609.5 x 62.3 x 0.51 mm. The plate is clad with aluminium 0.38 mm thick and the water gap between plates is 2.1 mm. This cladding thickness has been maintained in all calculations. As SILOE fuel elements also contain some 22.75 wt % alloy plates, the average ^{235}U per plate is reduced to 14.19 g in a typical core. Such variation in plate loading was not taken into account in this report.

The following parameter values have been used in the survey:

(a) 93, 40 and 20 per cent enrichment,

(b) 26 wt % and 45 wt % uranium in the fuel meat,

(c) 14.72, 10 and 7.36 g of ^{235}U per plate of area 609.5 x 62.3 mm^2, and

(d) 1.6, 2.1 and 2.6 mm water gap between plates.

The fuel plates and the labelling scheme used in this work are given in Table 1. Note that there is a large variation in meat thickness from 0.116 mm to 2.37 mm. Smaller thicknesses, although not very realistic, were included to produce a uniform table in which interpolation can be performed. In general, sufficient values for each parameter were included to allow linear interpolation between values. Interpolation methods are considered in a following section.

A minor difficulty arose with respect to the density of uranium-aluminium alloys achieved in fuel plates: there is a variation of about 10 per cent in the alloy densities calculated from nominal meat dimensions and ^{235}U loading quoted for various reactors; for example,

SILOE 26 wt % alloy is 9.5 per cent less than theoretical density,

OSIRIS 26 wt % alloy is 7.3 per cent less,

MTR 45 wt % alloy is 10 per cent less.

However, for fuel used by the AAEC, the data show that theoretical density is within 2 per cent for 16 to 25 per cent alloys. A uniform reduction of 9.5 per cent below theoretical density was used in this survey. Results for other densities may be obtained by a minor interpolation in the tables.

2.2 Power Normalisation

The power level at which any of the studied systems can be operated depends on heat transfer and coolant flow considerations. In order to present flux levels which are approximately correct, all results in this survey were normalised to the same average power per plate as that for SILOE at a power of 35 MW, i.e. 54.7 kW per plate of active dimensions 609.5 x 62.3 mm^2. The normalisation is thus to an average rating of 144 W per cm^2 of active plate area. (Results for other ratings may be obtained by a simple renormalisation.) This rating has also been used to include such quantities as the equilibrium xenon worth, but the changes in reactivity with rating are of little importance.

2.3 Major Assumptions

2.3.1 Type of calculation

The most important of the assumptions needed to reduce the computational effort to a reasonable amount concerns the reactor size, burnup and reflectors. The systems considered vary by about 20 per cent in reactivity so that the optimum configuration for each system also varies widely. Previous experience suggested that variation in flux levels with the range of critical core size was at least as significant as variation in flux levels with the type of fuel. The ability to interpolate between parameter values is also important but would be reduced if size, burnup and reflectors were varied between the calculated systems. Most results were therefore produced under the following assumptions.

(a) The reactor size is such that the power is 35 MW for the rating normalisation given in Section 2.2. This size is equivalent to 640 SILOE sized fuel plates, i.e. an active fuel plate area of 24.3 m^2.

(b) The average fuel burnup is 0.236 MWd/g of ^{235}U which corresponds to about 30 per cent destruction of the initial ^{235}U loading and also to 0.2487 fissions per initial fissile atom (FIFA).

(c) The calculation is performed in RZ geometry with an effectively infinite D_2O reflector. A diagram of the reactor layout used in the calculations is given in Figure 1. The principal features are:

(i) active core height of 609.5 mm,

(ii) variable core radius,

(iii) reflector width of 800 mm, and

(iv) reflector height of 1009.5 mm.

(d) The excess reactivity of the system was allowed to vary, but flux levels are quoted for a system poisoned to criticality with a thermal absorber uniformly distributed in the core.

The calculated reactivity can be taken as the excess reactivity at the end of a refuelling cycle for which the average discharge burnup is 2N/(N+1) times the average burnup in the calculation, where N is the number of refuelling batches. For a typical five-batch scheme the discharge burnup is 0.3933 MWd g^{-1}, that is, about 50 per cent ^{235}U destroyed or 0.4145 FIFA.

2.3.2 Core volume fractions

It is of considerable importance that the dilution of the reactor core, caused by such structure as the fuel element side plates, be represented in some reasonable fashion. If one considers only the fuelled portion of the elements (that is, slabs of fuel meat, cladding and water gap), a large overestimate of the fuel density and the water fraction of the core is made. Further dilution of the core is caused by the inclusion of irradiation elements and control elements. Typical values are given in the following table for which OSIRIS fuel element details were taken from a Commissariat a l'Energie Atomique report [1970].

VOLUME FRACTIONS

	Fuelled slabs SILOE & OSIRIS	Standard element SILOE	Standard element OSIRIS	Complete core SILOE
Fuel meat	0.151	0.117	0.110	0.102
Aluminium	0.226	0.358	0.366	0.358
Water	0.623	0.525	0.524	0.521
Sample	-	-	-	0.019

Whole core volume fractions are quite dependent on the type of control element and irradiation element employed.

It is certainly not desirable to attempt a fuel element design for each system studied, but the major features need to be included in some simple manner. The prescription used in this survey was based on SILOE fuel elements and the number of elements of each type in a typical 35 MW core. The main assumptions were:

(a) a fuelled slab volume fraction in standard elements of 0.7732,

(b) the ratio of fuel plates in various element types of standard: control:irradiation = 23:17:12,

(c) the ratio of the number of fuel elements of each type of standard:control:irradiation = 21:5:6, and

(d) MoO_3 sample volume fraction of irradiation elements of 0.1006.

Further details are given in Appendix A; of course, only the final core volume fractions are of real significance. The most interesting consequences of the assumptions are given below.

(a) For a given number of fuel plates, the core volume is proportional to the thickness of the fuel plate (t) plus the water gap (g). Thus for 640 fuel plates, the radius in the RZ model is given by $137.39\ \sqrt{(t+g)}$ mm.

(b) The volume fraction of the core occupied by water is given by $0.8028-0.7478\ t/(t+g)$.

(c) The volume fraction of the core assigned for irradiation experiments is a constant. The sample volume fraction is 0.019.

2.4 General Description of Calculation Method

The calculations have been performed using modules of the AUS reactor code scheme (Robinson 1975a). Full details of the calculations are given in Appendix A. The modules used were:

MIRANDA	a data preparation module which uses ENDFB/IV data,
ICPP	a collision probability module,
CHAR	a burnup module, and
POW	a 2D diffusion module.

Five-group cross section data for core materials were prepared from a cell burnup calculation using MIRANDA, ICPP and CHAR, in which the cell consisted of infinite slabs of fuel meat, cladding and water. This calculation was used to obtain data for H_2O and Al as well as for the

slab cell. Five-group reflector data were separately prepared. The boundaries of the five groups used throughout these calculations were:

0.82 MeV, 5.53 keV, 2.27 eV and 0.62 eV.

Four-group calculations with energy boundaries at 0.82 MeV, 5.53 keV and 0.62 eV are fairly standard in light water reactor calculations. An additional boundary has been included at 2.27 eV because this covers the range of upscattering in current AUS libraries.

Data for each element type were calculated in POW using a two-dimensional supercell calculation which included two standard elements, a control element and an irradiation element. This calculation merely gave fluxes for smearing the detail within a fuel element. Final core average cross sections were obtained by simple volume-smearing of fuel element types.

The final calculations were four five-group RZ diffusion calculations using the smeared core cross sections. Three of these were k_{eff} calculations to give the reactivity of the standard case having a burnup of 0.236 MWd g^{-1} and a power of 35 MW, the reactivity for a 20 per cent reduction in burnup to 0.1888 MWd g^{-1} and the reactivity for an increase in core size by 20 per cent to give a power of 42 MW. The fourth calculation was the standard case poisoned to criticality using a thermal (1/v) poison uniformly in the core. It was this last case for which fluxes, etc. are quoted.

2.5 Molybdenum Activity

In view of the importance of molybdenum activation the basis of the calculated activities is given in detail here. The samples were assumed to be of 20 mm diameter and to be natural molybdenum in the form of MoO_3 with a density of 1.5 g cm^{-3}. The shielded ^{98}Mo resonance integral calculated for this sample was 3.96 b. Other data used to obtain the activity were a thermal cross section of 0.13 b and a ^{98}Mo abundance of 24.4 per cent. The epithermal flux to be used with the resonance integral was taken from group 3 of the five-group set. No thermal flux depression or enhancement in the sample was included. The values quoted are saturated activities in curies per gram of molybdenum. In view of limited evidence, which suggests that the calculations underestimate activity, values could be taken as achievable activities.

2.6 Description of Tabulated and Graphical Results

2.6.1 Tabulated information

A large amount of information obtained from the survey calculations

is presented in Tables 2(a) to 5(c). The results for each value of the water gap have been grouped, the label A, B and C referring to 2.1, 1.6 and 2.6 mm water gap, respectively. Each type of fuel plate has been labelled by the three figure case number given in Table 1.

Reactivity information is given in Table 2, together with the volume fraction of the core which contains water and the core volume relative to the 93-26-14 case (93 per cent enrichment, 26 wt % uranium and 14.72 g of ^{235}U per plate) for a 2.1 mm water gap. This basic volume is 0.122 m^3. The reactivity unit used is:

$$\rho\% = 100(1-1/k_{eff}) \quad .$$

The reactivity information given is:

- the reactivity of the standard case which has a power of 35 MW and an average burnup of 0.236 MWd g^{-1},
- the change in reactivity when the burnup is reduced by 20 per cent, and
- the change in reactivity for a 20 per cent increase in core size.

Change in reactivity with burnup may be taken as linear over the range of interest, but for change of reactivity with core size, the following empirical relationship is recommended.

$$\rho(P) = \rho(35MW) + 8.35\ \Delta\rho(1-(35/P)^{0.7}) \quad ,$$

where $\rho(P)$ is the reactivity at power P for constant rating,
$\rho(35\ MW)$ is the tabulated reactivity for the standard case, and
$\Delta\rho$ is the tabulated reactivity change.

Tests have shown that this formula gives excellent results over a wide range of power.

The calculated radial and axial form factors are given in Table 3. The radial form factor is the peak-to-average value of the axial average fission rate. The axial form factor has been defined rather unusually as the peak point fission rate divided by the peak axial average fission rate. The axial form factor at zero radius has also been given. The axial form factor has a conventional meaning for the more undermoderated systems which have power peaks at the radial reflector boundary and for the more moderated systems which have power peaks at the core centre. However, for those systems for which the axial form factor is marked (*) the axial average fission rate has a peak value at the reflector boundary

while the point fission rate has a peak at the core centre. It must be emphasised that the radial form factor calculated is a macroscopic shape factor for uniform core loading. It is thus of limited interest, as the macroscopic shape changes with core loading and the power peaks within fuel elements and between different fuel elements are of major importance.

Thermal, fast and epithermal neutron flux are given in Tables 3 and 4. These descriptions have the meaning:

thermal - less than 0.62 eV,

fast - greater than 0.82 MeV, and

epithermal - between 5.53 keV and 2.27 eV.

Axial average values in these tables and also throughout this report refer to an axial average taken over the active core height.

The information of direct interest, that is, molybdenum activity and the reflector thermal flux peaks, is given in Table 5. Again, thermal is used to mean less than 0.62 eV.

2.6.2 Graphical information

The voluminous tabulated information has been presented in graphical form for a limited set of the more important information. Only the reactivity and the core average molybdenum activity have been given.

These results have been plotted against water fraction of the core in Figures 3, 4 and 5 for cases with ^{235}U content per plate of 14.72, 10 and 7.36 g, respectively. This is a convenient variable as most quantities are close to having a linear variation with water fraction for changes in enrichment, wt % uranium and water gap. In the reactivity figures, the curves drawn are for variation with water gap for a particular fuel type. The curves are labelled by two numbers giving the enrichment and the wt % uranium. On the activity figures, the results separate into a group for each water gap which has been labelled. Note that water fraction increases with an increase in any one of enrichment, wt % uranium, or water gap.

The variation with ^{235}U mass per plate is shown in Figure 6 for a 2.1 mm water gap. The results are plotted against the log of the mass with straight lines joining points which have the same enrichment and wt % uranium.

2.6.3 Interpolation in the tables

As indicated by Figures 3 to 6, linear interpolation in the water fraction corresponding to various enrichments and water gaps gives

adequate accuracy over the considered range of these parameters. Though only reactivity and average molybdenum activity are illustrated in the figures, the same is true for all calculated quantities. (Additionally, checks of interpolation in wt % uranium showed linear interpolation in water fraction to be adequate.)

For interpolation between values of the ^{235}U mass per plate, linear interpolation in log (mass) gives reasonable results. Interpolation to obtain reactivity gave the worst errors which may be as large as 0.4 per cent. If this is considered large for a simple interpolation error, quadratic interpolation may be used. Because the deviation from linearity is quite similar in all cases, the addition of the average quadratic term gives better than 0.1 per cent accuracy. The term is

0.94 a(a-1) for interpolation between 7.36 and 10 g, or

1.5 a(a-1) for interpolation between 10 and 14.72 g,

where a is the linear interpolation parameter, i.e.

$$a = \frac{\log M/7.36}{\log 10/7.36} \quad \text{or} \quad \frac{\log M/10}{\log 14.72/10} \quad .$$

2.6.4 Comments on the results

A few simple comments on the results are relevant at this point. Section 3 contains additional studies which will require further comments.

The reactivity of these well reflected systems is such that all cases are quite viable at ^{235}U plate loadings of 14.72 g; plate loadings as low as 10 g require 45 wt % uranium for 20 per cent enriched fuel; 40 per cent enriched fuel may be used with plate loadings as low as about 8.5 g, and fully enriched fuel may be used with all loadings considered. Fuel consumption rates are considered in Section 4.

For any values of the water gap and plate loading, the variation in the flux levels achieved with various fuel types is not large. A typical range of about 10 per cent was calculated for both Mo activity and reflector flux. As the variations in Mo activity and reflector flux are quite closely related for any change in the value of a parameter, there is no conflict between the two major requirements for the reactor. Molybdenum activity and reflector flux increase by about 20 per cent as the ^{235}U plate loading is reduced by a factor of two. The increased thermal flux in the core makes the most substantial contribution to the increased Mo activity. For most systems, the increase in average epithermal flux is only about 5 per cent for this loading change. The

Mo activity and reflector flux increase by about 30 per cent (at constant power per plate) as the water gap between plates is reduced from 2.6 to 1.6 mm. These results show that the flux levels achieved provide a considerable incentive for the use of low ^{235}U loadings and for reducing the water gap to the minimum consistent with hydraulic requirements.

For the 2.1 mm cases, the power normalisation is reasonable if SILOE coolant temperatures are achieved and the overall form factor is no worse than 2.4. Little evidence has been given here on the form factor which may be achieved. The axial form factor, which shows little variation, is perhaps the most useful information, but the radial form factor is simply a macroscopic shape factor. Even this macroscopic shape may be easily modified by, for example, loading new fuel in the centre of a system which has a core edge peak in a uniformly loaded core. Provided there are no gross flux distortions introduced through large differences in reflector effectiveness on different core faces, or large localised absorbers, an overall factor of 2.4 should be achievable. It may be necessary to use burnable poisons to reduce power peaking in new fuel elements.

For the 2.1 mm cases only, the largest value of the core average Mo activity is about 4.8 Ci g^{-1} for fully enriched fuel at 7.36 g plate loadings. The required value of 6 Ci g^{-1} is achieved for an axial average at the radial core centre. Reflector fluxes of 5×10^{14} neutrons cm^{-2} s^{-1} also require quite highly enriched fuel at the low plate loading. The reflector flux may be considerably modified by the precise core configuration.

3. ADDITIONAL INVESTIGATIONS

3.1 General

In this section the effects of a number of the assumptions made in Section 2 are investigated and some additional information given for specific systems. Unless otherwise specified, the investigation has been carried out for the case 93-26-14 at 2.1 mm water gap, which is the case closest to existing reactors. As these studies generally were made for the one case only, they must be regarded as illustrative of the resulting effects.

3.2 RZ Calculations of Various D_2O Reflectors

The survey calculations have a D_2O reflector which is 800 mm wide and extends axially 200 mm from the active core. The effects of reducing the reflector size are given in Table 6. The calculations used

here were k_{eff} calculations which included the thermal poison of the basic case. This calculation method results in an error, in the thermal flux in the core, of the same size as the change in reactivity. The calculations were for the same reactor layout as Figure 1, except that the top of the D_2O tank was included for those cases in which the reflector height was reduced.

The results in Table 6 show that core fluxes are not significantly affected by reducing the D_2O reflector to only 400 mm in thickness and to active core height. Though central flux and Mo activity increase by up to 4 per cent as the reflector size is reduced, core average fluxes increase by less than 1 per cent and, in particular, the variation in core average Mo activity is very small. The significant changes are in reactivity and peak reflector flux. The largest effects are obtained when the reflector height is reduced to that of the active core. The importance of the reduction in reactivity depends markedly on the system being considered. Neutron beam flux requirements in any system give a strong incentive for extending the reflector height to at least 100 mm and possibly 200 mm from the active core. The rather small changes calculated for a reduction from 800 mm to 600 mm wide suggest that 800 mm may be excessive.

3.3 RZ Calculations of Various Be Reflectors

The effects obtained by replacing the standard D_2O reflector by various Be reflectors were calculated in RZ geometry and are given in Table 7. The calculations were performed exactly as in Section 3.2. The investigation covers only the reflector width and the vol.% H_2O in the reflector. A reflector height equal to that of the active core was used throughout.

The results in Table 7 show that a width of 300 mm of Be is effectively infinite for both 10 and 20 per cent water cases. There is a significant gain in reactivity of 1.7 per cent from replacing the infinite D_2O reflector with Be and 10 per cent water, and a slight reduction if the reflector has 20 per cent water. Increases of 4 and 2 per cent in the average Mo activity for respectively 10 and 20 per cent water in the Be, are also of some significance.

3.4 XY Calculations

A series of calculations in XY geometry enable the effect of more practical geometric representations of the reactor to be studied. In these calculations the axial direction was represented by group and

material dependent bucklings obtained from the appropriate RZ calculations of the previous subsections. As the axial bucklings used were those corresponding to the active core height, the calculated fluxes are axial average values. The D_2O buckling was taken from the calculation with a 1009.5 mm high reflector. Again, k_{eff} calculations were used. The results obtained are given in Table 8.

In case 1, a square core with an 800 mm thick D_2O reflector on all sides was represented. The changes with respect to the RZ calculation are quite small, but the 5 per cent increase in the reflector flux at the core mid-face may be noted.

Case 2 has an 800 mm wide, D_2O reflector on one face of a square core and 90 per cent Be on the other three sides. The reflector layout is the same as that given in Figure 2, which shows the core and reflector layout for cases 4 and 5. Similar but smaller changes to those calculated for 90 per cent Be in RZ geometry are obtained in reactivity and core fluxes. However, a considerable flux tilt from south to north was introduced causing an 11 per cent reduction in the D_2O flux, compared to case 1 at the core midface.

In case 3, the effect of increasing the mesh size at the edge of the core is shown. In all previous calculations a fine mesh was used in the core at the reflector boundary. Such a mesh causes problem-size difficulties with an irregular core-reflector boundary. The effect of increasing the mesh to about 20 mm is shown in case 3, which is otherwise the same as case 2. The only significant change, which is in the radial form factor, is caused by a lack of definition in the flux at the core boundary. This indicates that the form factor is underestimated by about 7 per cent in the following cases.

In case 4, a plausible layout (Figure 2) for a core of 32 fuel elements was calculated. The core shape was chosen to maximise the flux in the D_2O reflector, to be suitable for a fixed reflector with irradiation facilities on the eastern side and to use Be blocks on the other sides. The D_2O flux is indeed increased by about 10 per cent, but the other main change is a 12 per cent deterioration in the form factor. This increase in form factor is caused by the irregular core boundary in the south-west corner where the peak occurs.

In case 5, the effect of representing individual fuel elements rather than using average core cross sections is shown. The fuel element layout is merely a plausible one. The main point is that fuel

element smearing has not caused a large reactivity error. Other interesting points are:

(a) the increase in the D_2O flux caused by concentrating irradiation elements in the south-west of the core,

(b) the reduction in form factor for the same reason as (a),

(c) the peak Mo activity of the smeared core is not achieved in the unsmeared core for a central irradiation element, and

(d) the average Mo activity in the irradiation elements as positioned is 3.7 per cent above the basic case core average and, excluding the two core edge positions, the increase is 9 per cent.

The following conclusions about the values given for the survey calculations in Tables 2 to 5 have been drawn from this study.

(a) No signficant reactivity error has been introduced through geometrical representation or fuel element smearing.

(b) Peak Mo activities are about 4 per cent higher than should be achieved in a uniformly loaded core.

(c) Average Mo activities are at least 5 per cent lower than should be achieved by careful element positioning.

(d) D_2O fluxes represent reasonable average figures, but peak values at least 10 per cent higher may be achieved at positions near the centre of the core face.

3.5 Core Size Effect

The effects on neutron flux of changing the core size from 35 MW are given in Table 9. Results for 20, 25 and 45 MW (at constant power per fuel plate) are given for the case 93-26-14 at 2.1 mm gap, and results at 45 MW for case 20-26-14 at 2.1 mm gap. Note first that the 45 MW values are essentially the same for both cases. This gives some confidence that the results are reasonably independent of the particular case studied. While the effects calculated are not particularly large, they are of the same order as the variation in neutron flux level with any one of the main parameters considered.

3.6 Burnup Effect

The effect on neutron flux of increasing the average core burnup by 20 per cent to 0.283 MWd/g of ^{235}U is given in the first column of Table 10. The main effect is an increase of 8 per cent in the average thermal flux in the core, corresponding to the 8 per cent decrease in the ^{235}U loading. As the change in epithermal flux is quite small, the effect of burnup on Mo activity is sensitive to the thermal component of the ^{98}Mo

reaction rate. Thus the Mo activity change would be almost doubled for 7.36 g per plate fuel.

3.7 Volume Fraction Assumptions

3.7.1 Dilute systems

Though the assumption of a constant volume fraction for overheads associated with fuel element side plates, irradiation elements, etc., is quite reasonable for survey calculations in which the fuel elements are not well defined, it in effect makes the irradiation volume proportional to the core volume. Thus the more dilute cores are penalised. The extent of this penalty was investigated by a calculation of the 20-26-14 case at 2.1 mm gap with the same irradiation volume as the standard case 93-26-14 at 2.1 mm gap. This results in a 3 per cent decrease in core volume, a 1.4 per cent increase in water fraction, a 0.7 per cent increase in reactivity and increases in neutron flux of the order of 1 per cent as shown in the third column of Table 10. The effects, which may be taken as proportional to the difference from unity of the relative core volume given in Table 2, are significant only in the slight reactivity increase for cores with 20 per cent enriched uranium.

3.7.2 Small cores

It will have been noted that, for fully reflected cores considered here, the fully enriched cases with large values of the ^{235}U mass per plate have sufficient reactivity to be operated at small core sizes corresponding to powers of 20 MW or less. For the standard case of 93-26-14 at 2.1 mm gap, a 20 MW core would have only 3.4 irradiation elements and 2.9 control elements of SILOE size if constant volume fractions were maintained. The results obtained for a 20 MW calculation with six irradiation elements and four control elements are given in the second column of Table 10. Comparison with Table 9 shows an additional 3 per cent reduction in average Mo activity and reflector flux, resulting from the different assumptions on volume fractions. The calculated reactivity of 6.9 per cent is 1.2 per cent lower than the constant volume fraction case. In practice, one would expect larger reductions in Mo activity in such a small core, simply because there are so few internal fuel elements.

3.8 Axial Reflector

The axial reflector used in the calculations was water and aluminium in volume ratio of one to one. This ratio was assumed without looking at possible detail in the axial direction. A calculation with

the composition changed to 60 per cent water showed negligible changes of -0.07 per cent in reactivity and changes of 0 to -0.5 per cent in flux levels.

3.9 Sample Worth

The reactivity worth of the Mo samples, included in all cases, is of some interest. Replacing the MoO_3 in all samples by Al resulted in only a 0.3 per cent increase in reactivity for the 93-26-14 case. An additional calculation with solid Al irradiation blocks instead of the standard mixture of Al, H_2O and MoO_3 resulted in no increase in reactivity over the with-sample case. Thus the rig burden for Mo irradiation is very small.

3.10 Fuel Element Smearing

Comparison of the effect of the supercell method used for smearing the detail within a fuel element with the simplest method of volume smearing shows that the supercell method gives 0.37 per cent lower reactivity than volume smearing.

3.11 Thermal Poison Worth

Values for the worth of a thermal (1/v) poison have been obtained from the calculations of k_{eff} and the poisoned-to-critical state. To a reasonable approximation, the values for 35 MW cores depend only on the ^{235}U mass per plate. The values are given in the following table.

^{235}U per plate (g)	ρ % per cm^2
14.72	0.012
10	0.017
7.36	0.022

3.12 Xenon Override

To place the calculated excess reactivity in context, an assessment of the xenon override requirements must be made. The results of calculations of per cent reactivity requirements are given in the following table.

Fuel	93-26-14	93-26-7
Water gap, mm	2.1	2.1
Equilibrium Xe worth (included)	3.4	3.4
½ h override	1.71	3.60
1 h override	3.26	6.88
2 h override	5.9	12.6
Total override	13.8	30.0

It can be seen that the reactivity needed is approximately inversely proportional to ^{235}U loading and that the requirements for low loading are quite severe.

3.13 Beam Tube Worth

Information on the reactivity worth of beam tubes is quite difficult to obtain from calculations as, essentially, a three-dimensional transport theory calculation is required. By transformation of geometry, the worth of a tube at the centre of the core face can be calculated in RZ geometry with the tube on the Z axis. This calculation has been performed using the two-dimensional discrete ordinate code DOT [Rhoades & Mynatt 1973] for a 6-inch diameter beam tube at the thermal flux peak for a case similar to 20-45-14 at 2.1 mm gap and a reactor size of 31 MW [B.J. McGregor, private communication]. The loss of reactivity calculated was 0.25 per cent. It may be inferred that the reactivity loss due to six beam tubes as envisaged should be less than 1.5 per cent.

4. CONCLUSIONS

This study was performed not to draw quantitative conclusions as to the relative performance of various fuel enrichments and the best way in which the fuels may be used, but rather to calculate a set of reactor physics information from which such conclusions can be drawn when thermal-hydraulic, economic and operational considerations are included. This section should be regarded as illustrative of the way the information in this report may be used and is primarily concerned with the calculation of fuel consumption rates for various configurations which were limited to cases with 2.1 mm water gap.

Excess reactivity requirements may be considered to have three components, namely, beam tube worth, rig requirements additional to those for Mo irradiation, and xenon override. If the nominal xenon override near the end of a fuel cycle is taken to be half an hour, and

if the beam tube worth is taken as 1.5 per cent for all systems, reasonable values for excess reactivity are 4, 5 and 6 per cent for 14.72, 10 and 7.36 g plates, respectively. Also some limit must be put on the discharge fuel burnup; in the following, this was 0.5 MWd/g of ^{235}U or 0.527 FIFA. Though the number of refuelling batches should be adjusted to give a reasonable fuel cycle length, the simple assumption of a five-batch scheme was made here.

From the above assumptions, together with the reactivity and the changes in reactivity with size and burnup for each case, fuel consumption rates may easily be calculated as a function of reactor power (at constant rating) for each case. The type of result obtained for fuel consumption rate, expressed as fuel plates per effective full power day (EFPD), is illustrated in Figure 7 for cases with a 2.1 mm water gap. In Figure 7, the fuel consumption rates for each value of the ^{235}U plate loading have a common straight line segment for which there is sufficient reactivity for the maximum burnup to be reached. The slope of these lines is simply inversely proportional to ^{235}U loading. The plate usage shown varies by a factor of ten even with the low loading and low enrichment cases omitted. The less reactive cases have very flat minima and the most reactive cases, which may be operated at very small core sizes, simply have minima for the smallest size for which the burnup takes the maximum value. Note that the results shown in Figure 7 involve large extrapolations from 35 MW calculations using reactivity variation with size for a constant volume fraction. This does not affect the trend of the results.

Further information on fuel cycles is given in Tables 11 and 12 for a power of 35 MW and the power at which fuel consumption is a minimum. The results may be converted to results for a three-batch refuelling scheme by increasing the fuel consumption rate by 11 per cent, decreasing the discharge burnup by 10 per cent and increasing the cycle length by 50 per cent. Also given in these tables is the average Mo activity for each case. The variation of Mo activity with size has been taken from Section 3.5 from which the empirical relationship

$$A(P)/A\ (35\ MW) = 1 + 0.4047\ [1-(35/P)^{\frac{1}{3}}]$$

was derived. The variation of Mo activity with burnup was taken from Section 3.6, assuming the change to be linear with burnup. The 5 per cent by which the average rig activity should exceed the core average

activity, as described in Section 3.4, was also applied. The most desirable configuration should lie between the 35 MW and the minimum fuel consumption tables for most cases.

In conclusion, the use of low enrichment fuel does not cause large reductions in the flux levels and Mo activity which may be achieved. It is most desirable that at least 45 wt % uranium alloy be adopted for 20 per cent enriched uranium. The fuel cost penalty associated with the use of low enrichment may be quite severe, particularly if low ^{235}U plate loadings are used to increase Mo activity.

5. REFERENCES

Commissariat a l'Energie Atomique [1970] - Reactor OSIRIS : descriptive report. CEA-R-3984.

Doherty, G. [1969] - Some methods of calculating first flight collision probabilities in slab and cylindrical lattices. AAEC/TM489.

International Atomic Energy Agency (IAEA) [1964] - Directory of nuclear reactors, Vol. V.

Merchie, F. [1971] - Engineering and use of research reactors at the Grenoble Nuclear Research Centre. Meeting on Research Reactor Utilization, Bandung. IAEA-147.

Pollard, J.P. [1974] - AUS module POW - a general purpose 0, 1 and 2D multigroup neutron diffusion code including feedback-free kinetics. AAEC/E269.

Rhoades, W.A. & Mynatt, F.R. [1973] - The DOTIII two-dimensional discrete ordinates transport code. ORNL-TM-4280.

Robinson, G.S. [1975a] - AUS - the Australian modular scheme for reactor neutronics computations. AAEC/E369.

Robinson, G.S. [1975b] - AUS burnup module CHAR and the associated STATUS data pool. AAEC/E372.

Robinson, G.S. [1977] - AUS module MIRANDA - a data preparation code based on multiregion resonance theory. AAEC/E410.

TABLE 1

CASE DESCRIPTION

Case	Enrichment wt %	Uranium wt %	^{235}U per plate g	Fuel meat thickness mm
93-26-14	93	26	14.72	0.51
40-26-14	40	26	14.72	1.1857
20-26-14	20	26	14.72	2.3715
93-45-14	93	45	14.72	0.2329
40-45-14	40	45	14.72	0.5415
20-45-14	20	45	14.72	1.0829
93-26-10	93	26	10	0.3465
40-26-10	40	26	10	0.8055
20-26-10	20	26	10	1.6111
93-45-10	93	45	10	0.1582
40-45-10	40	45	10	0.3678
20-45-10	20	45	10	0.7357
93-26-7	93	26	7.36	0.255
40-26-7	40	26	7.36	0.5929
20-26-7	20	26	7.36	1.1857
93-45-7	93	45	7.36	0.1164
40-45-7	40	45	7.36	0.2707
20-45-7	20	45	7.36	0.5415

TABLE 2(a)

REACTIVITY FOR 2.1 mm WATER GAP

Case	Water fraction of core	Relative core volume	Reactivity ρ%	Burnup effect Δρ%	Size effect Δρ%
93-26-14	0.5210	1	14.74	1.81	1.65
40-26-14	0.4432	1.201	8.76	1.93	1.68
20-26-14	0.3552	1.552	1.07	2.09	1.72
93-45-14	0.5627	0.918	16.21	1.73	1.63
40-45-14	0.5167	1.009	12.01	1.78	1.64
20-45-14	0.4533	1.170	7.20	1.84	1.65
93-26-10	0.5448	0.951	9.33	2.18	1.90
40-26-10	0.4834	1.088	4.13	2.24	1.94
20-26-10	0.4062	1.327	-2.88	2.36	2.00
93-45-10	0.5753	0.896	10.66	2.10	1.88
40-45-10	0.5415	0.958	7.10	2.08	1.89
20-45-10	0.4918	1.067	2.82	2.10	1.91
93-26-7	0.5591	0.924	2.96	2.63	2.17
40-26-7	0.5098	1.025	-1.69	2.63	2.21
20-26-7	0.4432	1.201	-8.21	2.71	2.28
93-45-7	0.5826	0.883	4.20	2.55	2.14
40-45-7	0.5566	0.929	1.10	2.48	2.15
20-45-7	0.5167	1.009	-2.81	2.45	2.18

TABLE 2(b)

REACTIVITY FOR 1.6 mm WATER GAP

Case	Water fraction of core	Relative core volume	Reactivity ρ%	Burnup effect Δρ%	Size effect Δρ%
93-26-14	0.4719	0.852	13.6	1.77	1.83
40-26-14	0.3925	1.052	6.99	1.92	1.84
20-26-14	0.3079	1.404	-1.26	2.07	1.85
93-45-14	0.5165	0.769	15.22	1.69	1.81
40-45-14	0.4674	0.861	10.49	1.76	1.80
20-45-14	0.4025	1.022	5.23	1.83	1.80
93-26-10	0.4971	0.803	9.14	2.07	2.10
40-26-10	0.4330	0.939	3.36	2.15	2.12
20-26-10	0.3563	1.178	-4.17	2.27	2.16
93-45-10	0.5301	0.747	10.58	1.98	2.07
40-45-10	0.4936	0.809	6.56	1.99	2.07
20-45-10	0.4415	0.919	1.88	2.02	2.08
93-26-7	0.5126	0.776	3.74	2.44	2.37
40-26-7	0.4602	0.876	-1.44	2.46	2.40
20-26-7	0.3925	1.052	-8.46	2.55	2.46
93-45-7	0.5382	0.735	5.08	2.36	2.34
40-45-7	0.5098	0.781	1.56	2.30	2.35
20-45-7	0.4674	0.861	-2.71	2.29	2.36

TABLE 2(c)

REACTIVITY FOR 2.6 mm WATER GAP

Case	Water fraction of core	Relative core volume	Reactivity ρ%	Burnup effect Δρ%	Size effect Δρ%
93-26-14	0.5574	1.148	14.88	1.88	1.53
40-26-14	0.4827	1.349	9.41	1.98	1.56
20-26-14	0.3942	1.701	2.18	2.13	1.62
93-45-14	0.5962	1.066	16.25	1.81	1.50
40-45-14	0.5534	1.158	12.46	1.83	1.52
20-45-14	0.4926	1.318	8.00	1.88	1.54
93-26-10	0.5796	1.100	8.56	2.32	1.77
40-26-10	0.5218	1.236	3.80	2.36	1.81
20-26-10	0.4461	1.475	-2.78	2.47	1.88
93-45-10	0.6076	1.044	9.80	2.25	1.74
40-45-10	0.5766	1.106	6.59	2.21	1.76
20-45-10	0.5297	1.215	2.62	2.22	1.79
93-26-7	0.5928	1.073	1.22	2.85	2.03
40-26-7	0.5469	1.173	-3.03	2.84	2.07
20-26-7	0.4827	1.349	-9.14	2.90	2.14
93-45-7	0.6143	1.032	2.38	2.77	2.00
40-45-7	0.5905	1.077	-0.40	2.69	2.02
20-45-7	0.5534	1.158	-4.01	2.64	2.05

TABLE 3(a)

FORM FACTORS AND CORE THERMAL FLUX FOR 2.1 mm WATER GAP

Case	Form Factors			Core Thermal Flux 10^{14} neutrons cm^{-2} s^{-1}		
	Radial	Axial	Axial at centre	Centre	Centre axial av.	Core av.
93-26-14	1.305	1.169	1.251	2.330	1.868	1.685
40-26-14	1.311	1.162	1.231	2.159	1.761	1.614
20-26-14	1.293	1.154	1.204	2.010	1.679	1.553
93-45-14	1.311	1.171	1.258	2.358	1.878	1.689
40-45-14	1.328	1.166	1.247	2.207	1.776	1.620
20-45-14	1.331	1.161	1.231	2.072	1.689	1.559
93-26-10	1.179	1.242*	1.264	3.421	2.711	2.358
40-26-10	1.186	1.207*	1.250	3.226	2.586	2.277
20-26-10	1.178	1.186*	1.230	3.045	2.481	2.203
93-45-10	1.183	1.245*	1.269	3.447	2.720	2.361
40-45-10	1.197	1.210*	1.261	3.273	2.601	2.283
20-45-10	1.201	1.186*	1.250	3.112	2.495	2.209
93-26-7	1.190	1.274	1.274	4.662	3.662	3.093
40-26-7	1.179	1.264	1.264	4.444	3.521	3.001
20-26-7	1.171	1.249	1.249	4.232	3.394	2.914
93-45-7	1.191	1.278	1.278	4.685	3.670	3.095
40-45-7	1.182	1.272	1.272	4.489	3.534	3.006
20-45-7	1.174	1.263	1.263	4.301	3.409	2.920

**Axial average fission rate has a peak value at the reflector boundary while the point fission rate has a peak at the core centre.*

TABLE 3(b)

FORM FACTORS AND CORE THERMAL FLUX FOR 1.6 mm WATER GAP

Case	Form Factors			Core Thermal Flux 10^{14} neutrons cm^{-2} s^{-1}		
	Radial	Axial	Axial at centre	Centre	Centre axial av.	Core av.
93-26-14	1.399	1.159	1.233	2.211	1.802	1.744
40-26-14	1.401	1.151	1.209	2.024	1.684	1.661
20-26-14	1.374	1.142	1.177	1.869	1.599	1.593
93-45-14	1.410	1.162	1.242	2.239	1.811	1.747
40-45-14	1.427	1.156	1.227	2.071	1.696	1.665
20-45-14	1.425	1.150	1.209	1.926	1.602	1.594
93-26-10	1.274	1.171	1.247	3.246	2.611	2.432
40-26-10	1.279	1.165	1.229	3.030	2.473	2.336
20-26-10	1.263	1.158	1.206	2.840	2.364	2.253
93-45-10	1.281	1.172	1.253	3.274	2.620	2.434
40-45-10	1.295	1.168	1.242	3.080	2.486	2.341
20-45-10	1.297	1.163	1.229	2.907	2.372	2.257
93-26-7	1.174	1.195*	1.257	4.419	3.521	3.178
40-26-7	1.180	1.175	1.244	4.177	3.363	3.070
20-26-7	1.172	1.169	1.226	3.952	3.230	2.972
93-45-7	1.179	1.197*	1.261	4.444	3.528	1.222
40-45-7	1.191	1.177	1.254	4.225	3.375	3.074
20-45-7	1.195	1.174	1.244	4.023	3.241	2.976

**Axial average fission rate has a peak value at the reflector boundary while the point fission rate has a peak at the core centre.*

TABLE 3(c)

FORM FACTORS AND CORE THERMAL FLUX FOR 2.6 mm WATER GAP

Case	Form Factors			Core Thermal Flux 10^{14} neutrons cm^{-2} s^{-1}		
	Radial	Axial	Axial at centre	Centre	Centre axial av.	Core av.
93-26-14	1.179	1.220*	1.264	2.428	1.925	1.647
40-26-14	1.230	1.179	1.246	2.271	1.827	1.585
20-26-14	1.219	1.163	1.222	2.127	1.746	1.529
93-45-14	1.226	1.225*	1.270	2.454	1.935	1.651
40-45-14	1.242	1.186*	1.260	2.317	1.843	1.591
20-45-14	1.246	1.169	1.247	2.190	1.761	1.536
93-26-10	1.216	1.277	1.277	3.568	2.798	2.312
40-26-10	1.204	1.264	1.264	3.388	2.683	2.240
20-26-10	1.196	1.247	1.247	3.215	2.582	2.172
93-45-10	1.218	1.281	1.281	3.591	2.806	2.315
40-45-10	1.208	1.274	1.274	3.433	2.698	2.246
20-45-10	1.199	1.264	1.264	3.281	2.599	2.180
93-26-7	1.249	1.287	1.287	4.866	3.785	3.040
40-26-7	1.240	1.278	1.278	4.666	3.656	2.959
20-26-7	1.232	1.264	1.264	4.463	3.533	2.878
93-45-7	1.250	1.290	1.290	4.887	3.791	3.042
40-45-7	1.242	1.284	1.284	4.708	3.668	2.964
20-45-7	1.235	1.277	1.277	4.529	3.549	2.885

**Axial average fission rate has a peak value at the reflector boundary while the point fission rate has a peak at the core centre.*

TABLE 4(a)

FAST AND EPITHERMAL FLUX FOR 2.1 mm WATER GAP

Case	Fast Flux 10^{14} neutrons cm^{-2} s^{-1}			Epithermal flux 10^{14} neutrons cm^{-2} s^{-1}		
	Centre	Centre axial av.	Core av.	Centre	Centre axial av.	Core av.
93-26-14	2.958	2.302	1.727	2.612	2.032	1.604
40-26-14	2.676	2.104	1.593	2.440	1.915	1.521
20-26-14	2.313	1.842	1.406	2.237	1.775	1.410
93-45-14	3.080	2.388	1.789	2.673	2.072	1.635
40-45-14	2.916	2.275	1.719	2.560	1.996	1.585
20-45-14	2.685	2.111	1.606	2.429	1.906	1.518
93-26-10	3.124	2.415	1.779	2.744	2.121	1.648
40-26-10	2.912	2.268	1.683	2.609	2.031	1.585
20-26-10	2.618	2.059	1.535	2.442	1.918	1.498
93-45-10	3.212	2.477	1.824	2.789	2.152	1.671
40-45-10	3.093	2.396	1.775	2.701	2.093	1.633
20-45-10	2.919	2.274	1.693	2.597	2.022	1.583
93-26-7	3.254	2.502	1.816	2.841	2.187	1.676
40-26-7	3.087	2.387	1.741	2.732	2.114	1.626
20-26-7	2.844	2.216	1.623	2.592	2.019	1.555
93-45-7	3.319	2.548	1.848	2.875	2.209	1.692
40-45-7	3.229	2.488	1.813	2.805	2.162	1.663
20-45-7	3.091	2.391	1.750	2.719	2.104	1.622

TABLE 4(b)

FAST AND EPITHERMAL FLUX FOR 1.6 mm WATER GAP

Case	Fast Flux 10^{14} neutrons cm^{-2} s^{-1}			Epithermal Flux 10^{14} neutrons cm^{-2} s^{-1}		
	Centre	Centre axial av.	Core av.	Centre	Centre axial av.	Core av.
93-26-14	3.377	2.654	2.046	3.017	2.368	1.929
40-26-14	2.996	2.382	1.857	2.790	2.212	1.811
20-26-14	2.527	2.038	1.602	2.528	2.025	1.655
93-45-14	3.551	2.779	2.138	3.105	2.428	1.978
40-45-14	3.320	2.617	2.033	2.951	2.323	1.904
20-45-14	3.008	2.392	1.873	2.779	2.202	1.809
93-26-10	3.585	2.798	2.121	3.186	2.486	1.995
40-26-10	3.292	2.591	1.979	3.003	2.361	1.903
20-26-10	2.902	2.309	1.774	2.783	2.207	1.778
93-45-10	3.710	2.887	2.186	3.249	2.529	2.030
40-45-10	3.542	2.771	2.113	3.130	2.447	1.975
20-45-10	3.301	2.599	1.994	2.990	2.350	1.901
93-26-7	3.741	2.905	2.169	3.306	2.567	2.035
40-26-7	3.509	2.743	2.060	3.157	2.466	1.962
20-26-7	3.183	2.509	1.893	2.971	2.338	1.860
93-45-7	3.837	2.973	2.218	3.356	2.601	2.062
40-45-7	3.708	2.885	2.165	3.259	2.535	2.018
20-45-7	3.516	2.749	2.072	3.143	2.455	1.959

TABLE 4(c)

FAST AND EPITHERMAL FLUX FOR 2.6 mm WATER GAP

Case	Fast Flux 10^{14} neutrons cm^{-2} s^{-1}			Epithermal Flux 10^{14} neutrons cm^{-2} s^{-1}		
	Centre	Centre axial av.	Core av.	Centre	Centre axial av.	Core av.
93-26-14	2.640	2.040	1.495	2.313	1.788	1.373
40-26-14	2.423	1.890	1.397	2.179	1.698	1.312
20-26-14	2.135	1.684	1.253	2.017	1.588	1.229
93-45-14	2.732	2.104	1.540	2.360	1.818	1.396
40-45-14	2.608	2.020	1.490	2.272	1.760	1.359
20-45-14	2.431	1.895	1.406	2.169	1.690	1.310
93-26-10	2.780	2.134	1.536	2.422	1.861	1.405
40-26-10	2.619	2.024	1.465	2.319	1.792	1.360
20-26-10	2.390	1.863	1.355	2.188	1.705	1.296
93-45-10	2.845	2.179	1.567	2.456	1.883	1.421
40-45-10	2.757	2.120	1.533	2.389	1.838	1.394
20-45-10	2.625	2.029	1.473	2.308	1.785	1.357
93-26-7	2.889	2.207	1.563	2.502	1.913	1.424
40-26-7	2.765	2.122	1.510	2.420	1.859	1.389
20-26-7	2.579	1.994	1.423	2.312	1.788	1.338
93-45-7	2.938	2.241	1.586	2.528	1.930	1.436
40-45-7	2.871	2.196	1.561	2.474	1.894	1.415
20-45-7	2.769	2.126	1.517	2.409	1.852	1.386

TABLE 5(a)

MOLYBDENUM ACTIVITY AND REFLECTOR FLUX FOR 2.1 mm WATER GAP

Case	Molybdenum Activity Ci* g^{-1}			Reflector Thermal Flux 10^{14} neutrons cm^{-2} s^{-1}	
	Peak	Peak axial av.	Core av.	Peak	Peak axial av.
93-26-14	6.407	5.005	4.027	4.330	3.742
40-26-14	5.968	4.709	3.817	4.139	3.584
20-26-14	5.473	4.372	3.551	3.846	3.338
93-45-14	6.549	5.096	4.095	4.401	3.801
40-45-14	6.245	4.890	3.958	4.299	3.718
20-45-14	5.908	4.660	3.788	4.130	3.578
93-26-10	7.157	5.560	4.416	4.759	4.089
40-26-10	6.785	5.311	4.243	4.608	3.966
20-26-10	6.348	5.018	4.020	4.373	3.772
93-45-10	7.266	5.629	4.466	4.810	4.130
40-45-10	7.003	5.450	4.350	4.723	4.061
20-45-10	6.709	5.252	4.207	4.588	3.950
93-26-7	7.909	6.117	4.801	5.171	4.427
40-26-7	7.578	5.896	4.651	5.044	4.325
20-26-7	7.181	5.632	4.455	4.850	4.165
93-45-7	7.992	6.168	4.838	5.206	4.456
40-45-7	7.756	6.008	4.735	5.131	4.396
20-45-7	7.485	5.825	4.606	5.016	4.302

* 1 Ci = 3.7×10^{10} Bq

TABLE 5(b)

MOLYBDENUM ACTIVITY AND REFLECTOR FLUX FOR 1.6 mm WATER GAP

Case	Molybdenum Activity Ci* g^{-1}			Reflector Thermal Flux 10^{14} neutrons cm^{-2} s^{-1}	
	Peak	Peak axial av.	Core av.	Peak	Peak axial av.
93-26-14	7.185	5.664	4.710	5.126	4.440
40-26-14	6.627	5.280	4.419	4.844	4.206
20-26-14	6.005	4.846	4.056	4.433	3.859
93-45-14	7.384	5.796	4.815	5.240	4.536
40-45-14	6.989	5.523	4.622	5.079	4.404
20-45-14	6.562	5.227	4.388	4.835	4.200
93-26-10	7.980	6.255	5.145	5.615	4.839
40-26-10	7.499	5.928	4.904	5.388	4.654
20-26-10	6.947	5.549	4.597	5.053	4.374
93-45-10	8.128	6.352	5.221	5.694	4.904
40-45-10	7.791	6.120	5.061	5.563	4.798
20-45-10	7.418	5.863	4.864	5.364	4.635
93-26-7	8.742	6.823	5.558	6.090	5.230
40-26-7	8.318	6.536	5.350	5.903	5.078
20-26-7	7.820	6.198	5.084	5.624	4.848
93-45-7	8.859	6.898	5.616	6.149	5.279
40-45-7	8.557	6.691	5.475	6.036	5.189
20-45-7	8.220	6.459	5.302	5.870	5.052

* 1 Ci = 3.7×10^{10} Bq

TABLE 5(c)

MOLYBDENUM ACTIVITY AND REFLECTOR FLUX FOR 2.6 mm WATER GAP

Case	Molybdenum Activity Ci* g^{-1}			Reflector Thermal Flux 10^{14} neutrons cm^{-2} s^{-1}	
	Peak	Peak axial av.	Core av.	Peak	Peak axial av.
93-26-14	5.838	4.531	3.543	3.756	3.238
40-26-14	5.484	4.295	3.383	3.617	3.126
20-26-14	5.076	4.022	3.179	3.400	2.944
93-45-14	5.950	4.601	3.594	3.807	3.280
40-45-14	5.704	4.435	3.488	3.732	3.221
20-45-14	5.429	4.250	3.358	3.610	3.121
93-26-10	6.568	5.068	3.906	4.143	3.551
40-26-10	6.267	4.870	3.774	4.035	3.464
20-26-10	5.909	4.635	3.604	3.864	3.323
93-45-10	6.651	5.120	3.942	4.178	3.580
40-45-10	6.438	4.977	3.852	4.116	3.530
20-45-10	6.197	4.816	3.742	4.018	3.451
93-26-7	7.312	5.618	4.272	4.507	3.849
40-26-7	7.046	5.443	4.158	4.418	3.777
20-26-7	6.722	5.231	4.009	4.279	3.664
93-45-7	7.378	5.658	4.300	4.532	3.870
40-45-7	7.183	5.526	4.217	4.477	3.825
20-45-7	6.962	5.378	4.119	4.395	3.760

* 1 Ci = 3.7×10^{10} Bq

TABLE 6

RZ CALCULATIONS WITH VARIOUS D_2O REFLECTORS

(Per cent difference from basic case of 800 mm wide 1009.5 mm high)

Reflector width (mm)	600	400	800	600	400	800
Reflector height (mm)	1009.5	1009.5	609.5	609.5	609.5	809.5
Reactivity, ρ%	-0.17	-0.69	-1.59	-1.65	-1.89	-0.44
Form factors:						
Radial	-0.9	-3.6	-7.0	-7.3	-8.5	-2.3
Axial	+0.1	+0.4	+4.2*	+4.6*	+6.8*	+0.9
Axial at centre	0	+0.1	+0.8	+0.8	+0.8	+0.2
Core thermal flux:						
Centre	+0.3	+1.3	+3.6	+3.7	+4.2	+1.0
Centre axial average	+0.3	+1.2	+2.7	+2.8	+3.3	+0.8
Average	-0.2	-0.8	-1.8	-1.8	-2.1	-0.5
Core fast flux:						
Centre	+0.4	+1.6	+4.3	+4.4	+5.0	+1.1
Centre axial average	+0.3	+1.5	+3.6	+3.7	+4.2	+1.0
Average	+0.1	+0.4	+0.9	+1.0	+1.1	+0.3
Core epithermal flux:						
Centre	+0.3	+1.4	+3.8	+3.9	+4.4	+1.0
Centre axial average	+0.3	+1.3	+3.0	+3.1	+3.6	+0.9
Average	+0.1	+0.3	+0.4	+0.4	+0.5	+0.2
Molybdenum activity:						
Centre	+0.3	+1.4	+3.8	+3.9	+4.3	+1.0
Centre axial average	+0.3	+1.3	+3.0	+3.1	+3.5	+0.9
Average	0	+0.1	0	0	+0.1	+0.1
Reflector thermal flux:						
Peak	-2.2	-8.0	-10.5	-11.1	-14.1	-3.6
Peak axial average	-2.4	-8.7	-15.8	-16.5	-19.3	-5.3

**Axial average fission rate has a peak value at the reflector boundary while the point fission rate has a peak at the core centre.*

TABLE 7

RZ CALCULATIONS WITH VARIOUS Be REFLECTORS

(Per cent difference from basic case of 800 mm wide, 1009.5 mm high, D_2O reflector)

Be/H_2O mixture Reflector width (mm)	90% Be 400	90% Be 300	90% Be 200	80% Be 300	80% Be 200
Reactivity, ρ%	+1.75	+1.73	+1.54	-0.19	-0.27
Form factors:					
Radial	-6.5	-6.6	-7.5	-7.7	-8.1
Axial	+9.9	+9.9	+9.8	+10.3	+10.2
Axial at centre	+1.6	+1.6	+1.6	+1.6	+1.6
Core thermal flux:					
Centre	+3.6	+3.6	+3.9	+4.9	+5.1
Centre axial average	+1.9	+1.9	+2.2	+3.3	+3.4
Average	+1.5	+1.5	+1.2	-0.4	-0.5
Core fast flux:					
Centre	+2.7	+2.8	+3.1	+4.9	+5.2
Centre axial average	+1.2	+1.2	+1.6	+3.5	+3.6
Average	+4.3	+4.3	+4.4	+4.0	+4.0
Core epithermal flux:					
Centre	+3.3	+3.4	+3.7	+5.0	+5.1
Centre axial average	+1.8	+1.8	+2.2	+3.4	+3.6
Average	+4.6	+4.6	+4.6	+2.1	+2.2
Molybdenum activity:					
Centre	+3.4	+3.4	+3.7	+5.0	+5.1
Centre axial average	+1.8	+1.9	+2.2	+3.4	+3.5
Average	+4.1	+4.1	+4.1	+1.8	+1.8
Reflector thermal flux:					
Peak	-4.7	-5.0	-7.7	-6.7	-7.9
Peak axial average	-14.4	-14.7	-17.0	-16.8	-17.8

TABLE 8

XY CALCULATIONS

(Percentage difference from basic case of D_2O reflector in RZ geometry)

Case No. Core shape Reflector Mesh spacing Fuel elements smeared	1 square D_2O small yes	2 square D_2O & 90% Be small yes	3 square D_2O & 90% Be large yes	4 rectangular D_2O & 90% Be large yes	5 rectangular D_2O & 90% Be large no
Reactivity, ρ%	-0.23	+0.74	+0.81	+0.64	+0.14
Radial form factor	-0.5	+2.6	-4.2	+8.4	+2.7
Core thermal flux:					
Peak	-1.2	+1.5	+1.3	+0.6	-0.4†
Average	-0.2	+0.5	+0.6	+0.5	+0.6
Core fast flux:					
Peak	-1.0	+1.6	+1.3	+0.7	-9.4†
Average	-1.3	+2.3	+2.1	+1.2	+0.2
Core epithermal flux:					
Peak	-0.7	+2.1	+1.9	+1.2	-4.6†
Average	-0.7	+2.8	+2.7	+2.1	+1.4
Molybdenum activity:					
Peak	-0.8	+2.0	+1.8	+1.1	-4.0†
Average	-0.6	+2.5	+2.4	+1.9	+1.3
Reflector thermal flux peaks:					
1. mid-side in D_2O	+5.3	-5.4	-5.9	+4.7	+12.3
2. north-east corner in D_2O	-5.6	-23.0	-22.0	-18.2	-10.3
3. east mid-side in Be		-4.2	-4.7	-9.7	-4.8
4. south mid-side in Be		-3.3	-3.8	-4.3	-12.7

†Value is for central irradiation element

TABLE 9

CORE SIZE EFFECT

(Percentage difference from basic case with power of 35 MW)

Case	93-26-14 at 2.1 mm gap			20-26-14 at 2.1 mm gap
Power, MW	20	25	45	45
Form factors:				
Radial	+1.0	+1.0	-1.5	-1.2
Axial	0	0	0	0
Axial at centre	-0.6	-0.3	+0.2	0
Core thermal flux:				
Centre	-7.8	-4.8	+3.7	+3.7
Centre axial average	-7.3	-4.5	+3.5	+3.6
Average	+0.9	+0.5	-0.4	-0.3
Core fast flux:				
Centre	-12.5	-7.5	+5.5	+5.1
Centre axial average	-11.9	-7.3	+5.3	+5.0
Average	-9.6	-5.6	+3.8	+3.6
Core epithermal flux:				
Centre	-14.2	-8.6	+6.3	+6.0
Centre axial average	-13.7	-8.3	+6.1	+5.9
Average	-10.0	-5.8	+3.9	+3.8
Molybdenum activity:				
Centre	-13.3	-8.1	+5.9	+5.7
Centre axial average	-12.8	-7.8	+5.8	+5.6
Average	-8.3	-4.8	+3.2	+3.2
Reflector thermal flux:				
Peak	-5.6	-3.1	+1.5	+1.4
Peak axial average	-5.9	-3.3	+1.5	+1.5

TABLE 10

MISCELLANEOUS EFFECTS
(Percentage difference from basic case)

Case	93-26-14 at 2.1 mm gap	93-26-14 at 2.1 mm gap	20-26-14 at 2.1 mm gap
Change	20% increase in burnup i.e. 0.283 MWd/g ^{235}U	Power of 20 MW, 6 irradiation elements, 4 control elements	Irradiation volume as for 93-26-14 at 2.1 mm gap
Form factors:			
Radial	-2.3	-0.8	+0.7
Axial	+0.2	0	-0.1
Axial at centre	+0.1	-0.7	+0.1
Core thermal flux:			
Centre	+9.0	-6.5	-0.4
Centre axial average	+8.8	-5.9	-0.5
Average	+8.0	+1.5	-0.2
Core fast flux:			
Centre	+0.6	-16.2	+1.8
Centre axial average	+0.5	-15.7	+1.7
Average	+0.2	-13.7	+1.8
Core epithermal flux:			
Centre	+0.7	-17.2	+1.4
Centre axial average	+0.6	-16.7	+1.3
Average	+0.3	-13.4	+1.5
Molybdenum activity:			
Centre	+1.8	-15.8	+1.2
Centre axial average	+1.7	-15.2	+1.1
Average	+1.5	-11.2	+1.2
Reflector thermal flux:			
Peak	+1.7	-8.5	+1.3
Peak axial average	+1.6	-8.7	+1.3

TABLE 11

FUEL CYCLE INFORMATION AND MOLYBDENUM ACTIVITY AT 35 MW

Case	Fuel Plates per EFPD	Av. Discharge Burnup MWd g^{-1}	Fuel Cycle Length days	Reactivity ρ%	Av. Mo Activity Ci* g^{-1}
93-26-14	4.8	0.50	26.9	12.3	4.31
40-26-14	4.8	0.50	26.9	6.1	4.09
20-26-14	8.4	0.28	15.2	4.0	3.65
93-45-14	4.8	0.50	26.9	13.9	4.39
40-45-14	4.8	0.50	26.9	9.6	4.24
20-45-14	4.8	0.50	26.9	4.7	4.06
93-26-10	7.0	0.50	18.3	6.4	4.73
40-26-10	9.6	0.36	13.3	5.0	4.43
20-26-10	26.8	0.13	4.8	5.0	4.01
93-45-10	7.0	0.50	18.3	7.8	4.78
40-45-10	7.4	0.47	17.3	5.0	4.64
20-45-10	11.2	0.31	11.4	5.0	4.35
93-26-7	15.7	0.30	8.1	6.0	4.95
40-26-7	29.1	0.16	4.4	6.0	4.67
20-26-7	-				
93-45-7	14.1	0.34	9.1	6.0	5.03
40-45-7	20.0	0.24	6.4	6.0	4.82
20-45-7	43.1	0.11	3.0	6.0	4.58

* 1 Ci = 3.7×10^{10} Bq

TABLE 12

FUEL CYCLE INFORMATION AND MOLYBDENUM ACTIVITY FOR MINIMUM FUEL CONSUMPTION

Case	Power MW	Fuel Plates per EFPD	Av. Discharge Burnup MWd g^{-1}	Fuel Cycle Length days	Av. Mo. Activity Ci* g^{-1}
93-26-14	17.5	2.4	0.49	26.2	3.85
40-26-14	27.0	3.9	0.47	25.5	3.92
20-26-14	41.0	8.2	0.34	18.3	3.77
93-45-14	16.0	2.2	0.50	26.8	3.86
40-45-14	21.5	2.9	0.50	26.9	3.94
20-45-14	30.0	4.4	0.46	24.9	3.94
93-26-10	28.5	6.2	0.46	16.9	4.56
40-26-10	37.0	9.6	0.38	14.1	4.48
20-26-10	55.5	19.5	0.28	10.4	4.37
93-45-10	27.0	5.5	0.49	17.9	4.60
40-45-10	32.5	7.4	0.44	16.1	4.56
20-45-10	41.0	11.0	0.37	13.7	4.49
93-26-7	39.5	15.5	0.35	9.3	5.08
40-26-7	51.5	23.8	0.29	7.9	5.03
20-26-7	70.0	49.2	0.19	5.2	4.87
93-45-7	37.5	14.0	0.36	9.8	5.10
40-45-7	45.5	18.5	0.33	9.0	5.08
20-45-7	58.5	27.7	0.29	7.7	5.04

* 1 Ci = 3.7×10^{10} Bq

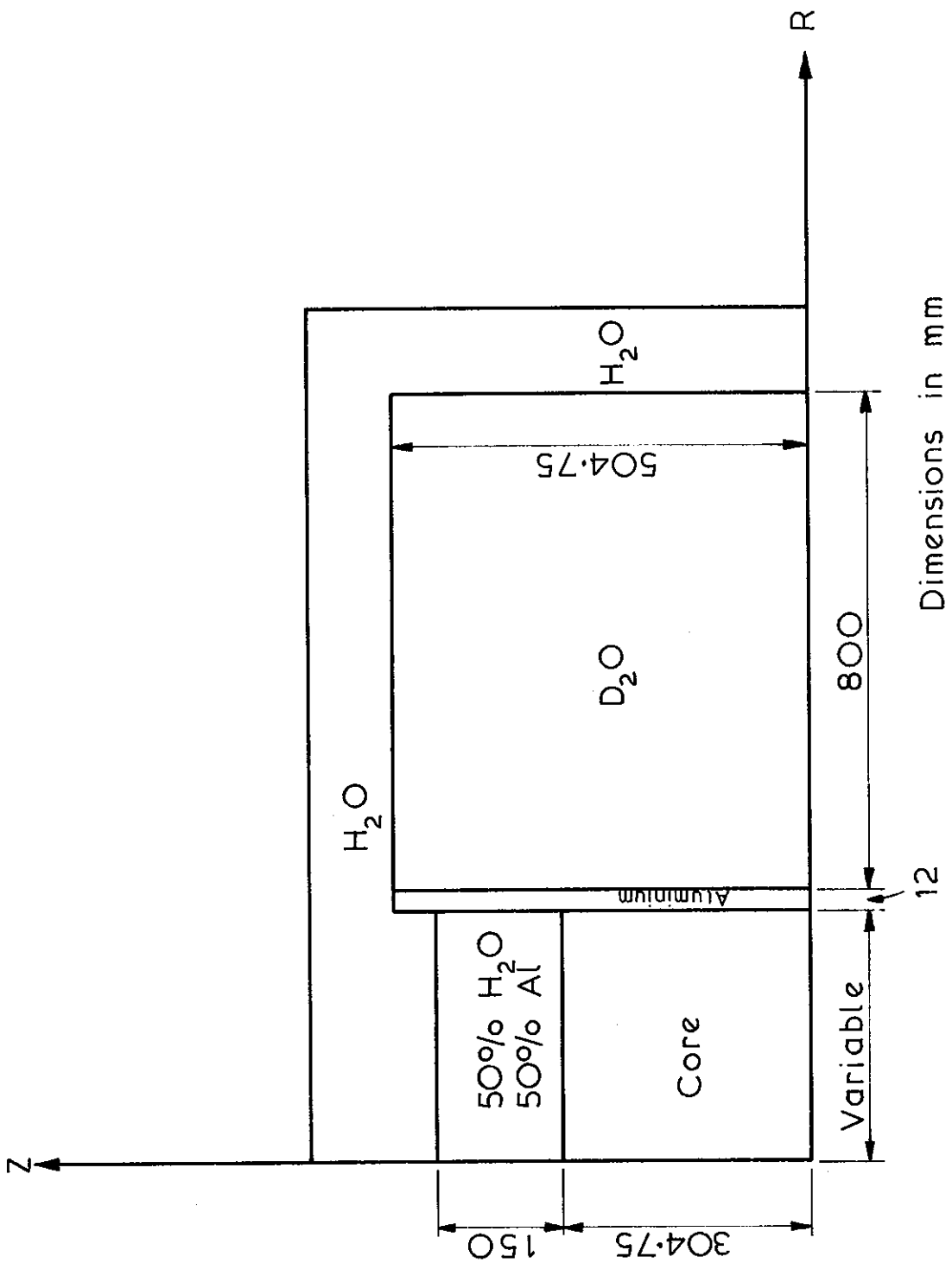

FIGURE 1. RZ GEOMETRY LAYOUT

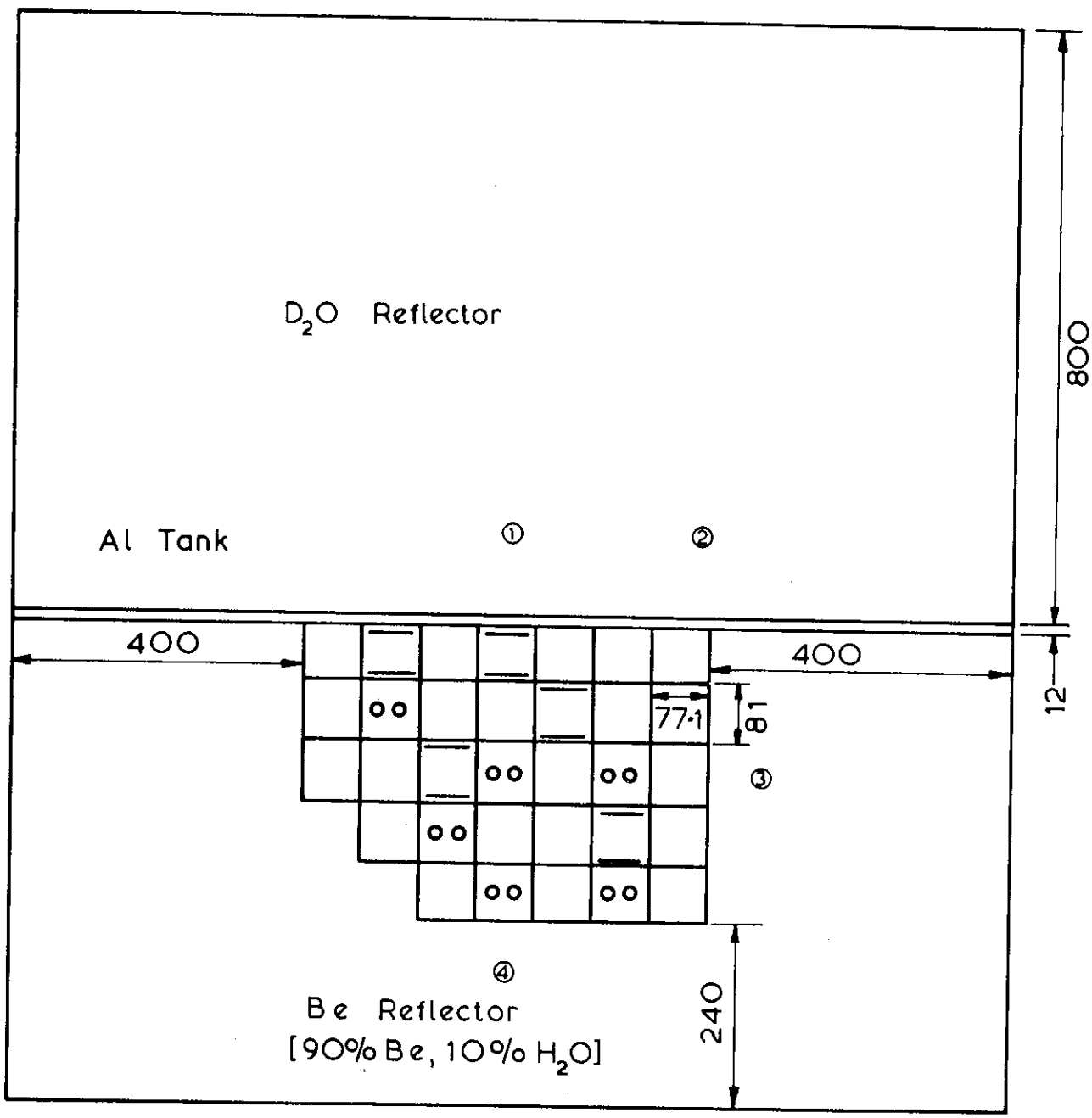

FIGURE 2. XY RECTANGULAR LAYOUT

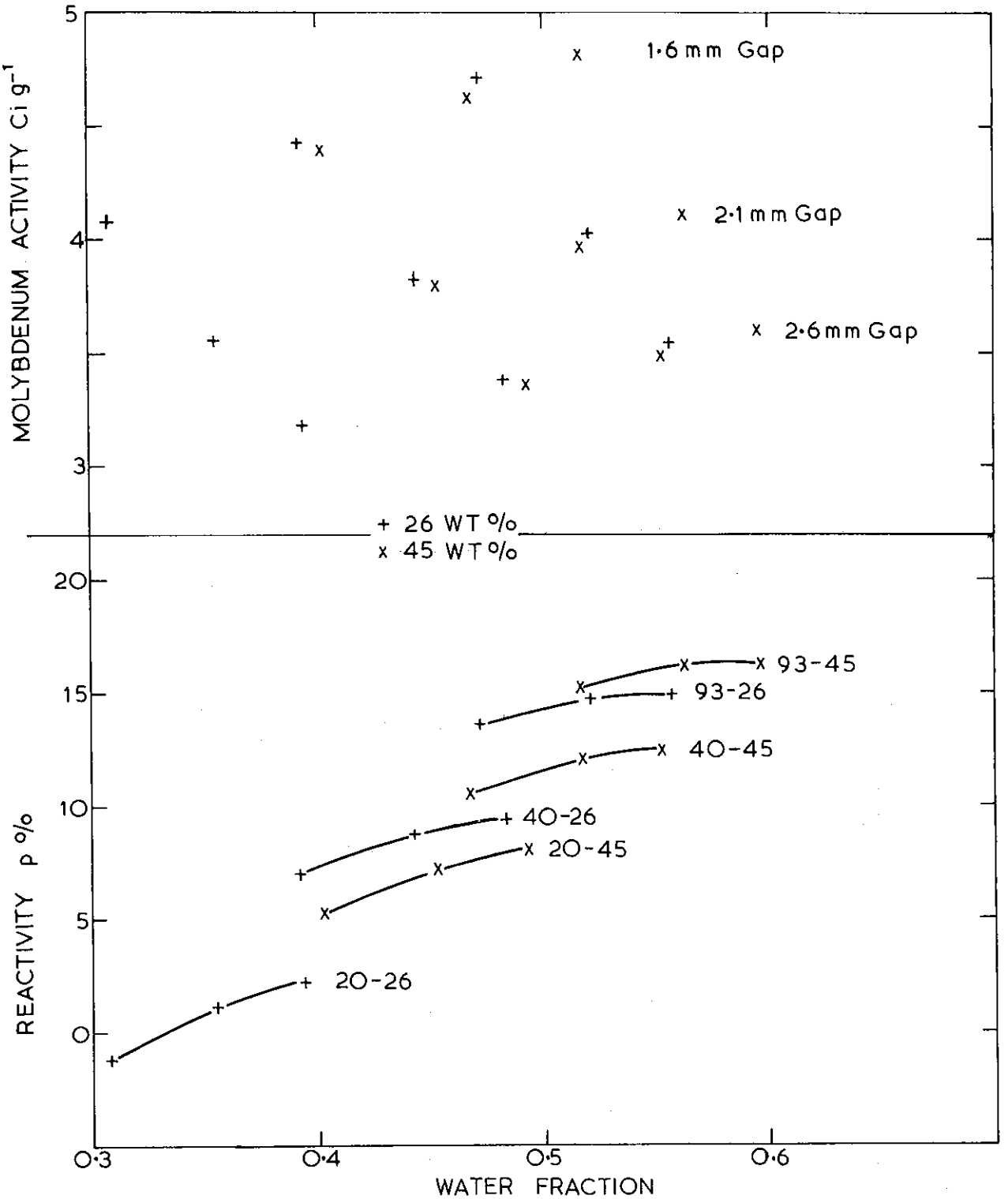

FIGURE 3. 14.72 g PER PLATE MOLYBDENUM ACTIVITY AND REACTIVITY

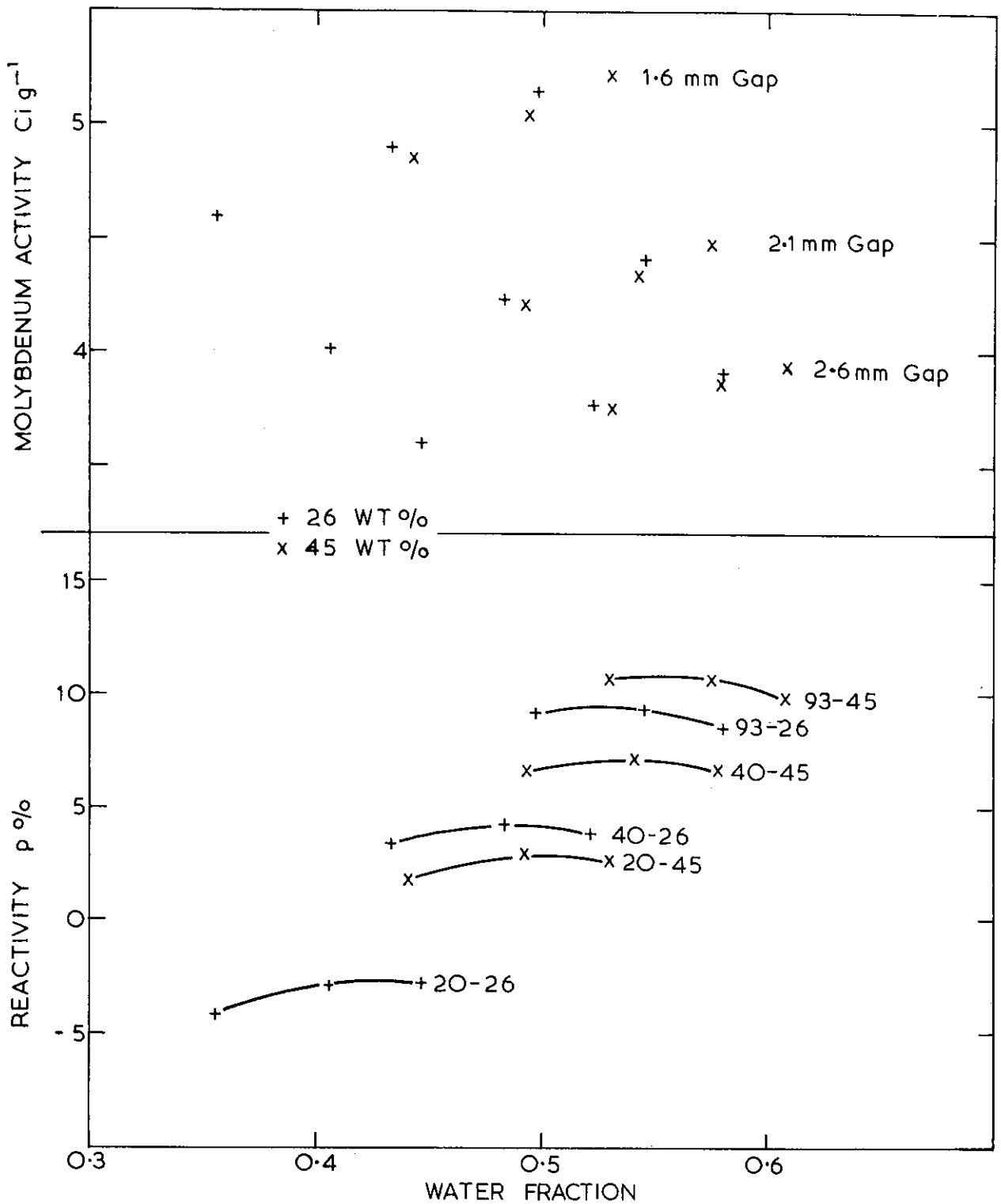

FIGURE 4. 10 g PER PLATE MOLYBDENUM ACTIVITY AND REACTIVITY

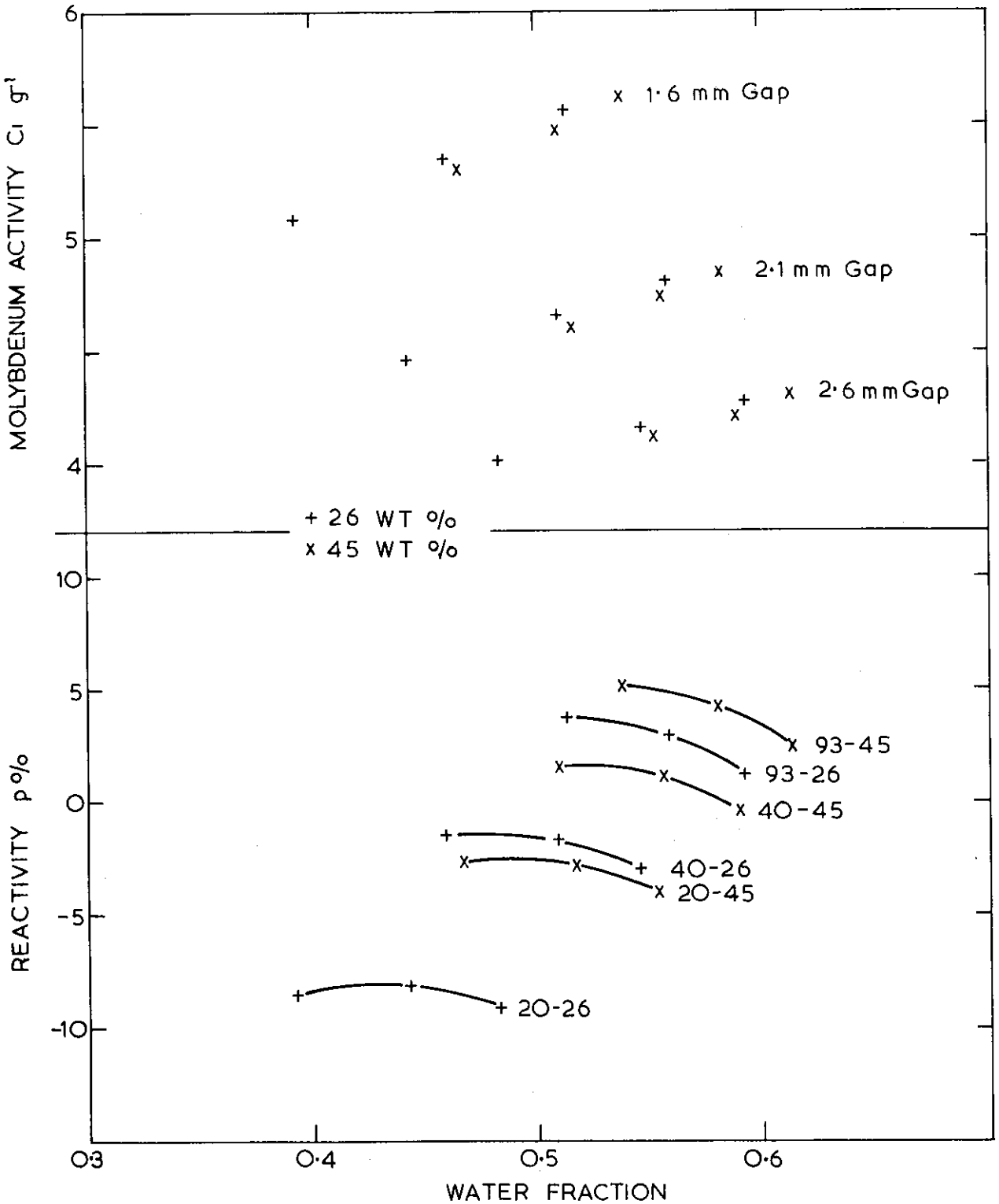

FIGURE 5. 7.36 g PER PLATE MOLYBDENUM ACTIVITY AND REACTIVITY

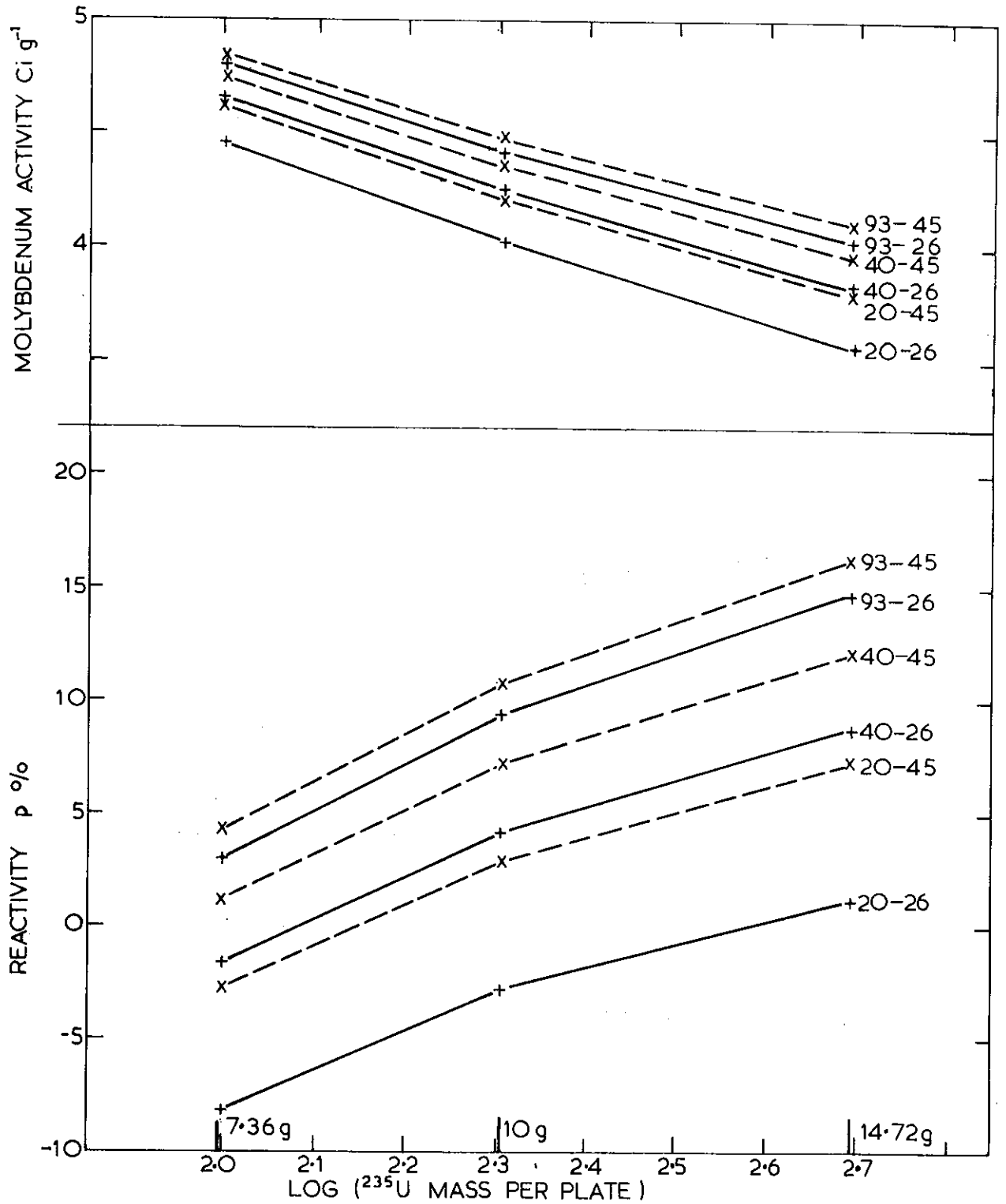

FIGURE 6. 2.1 mm WATER GAP MOLYBDENUM ACTIVITY AND REACTIVITY

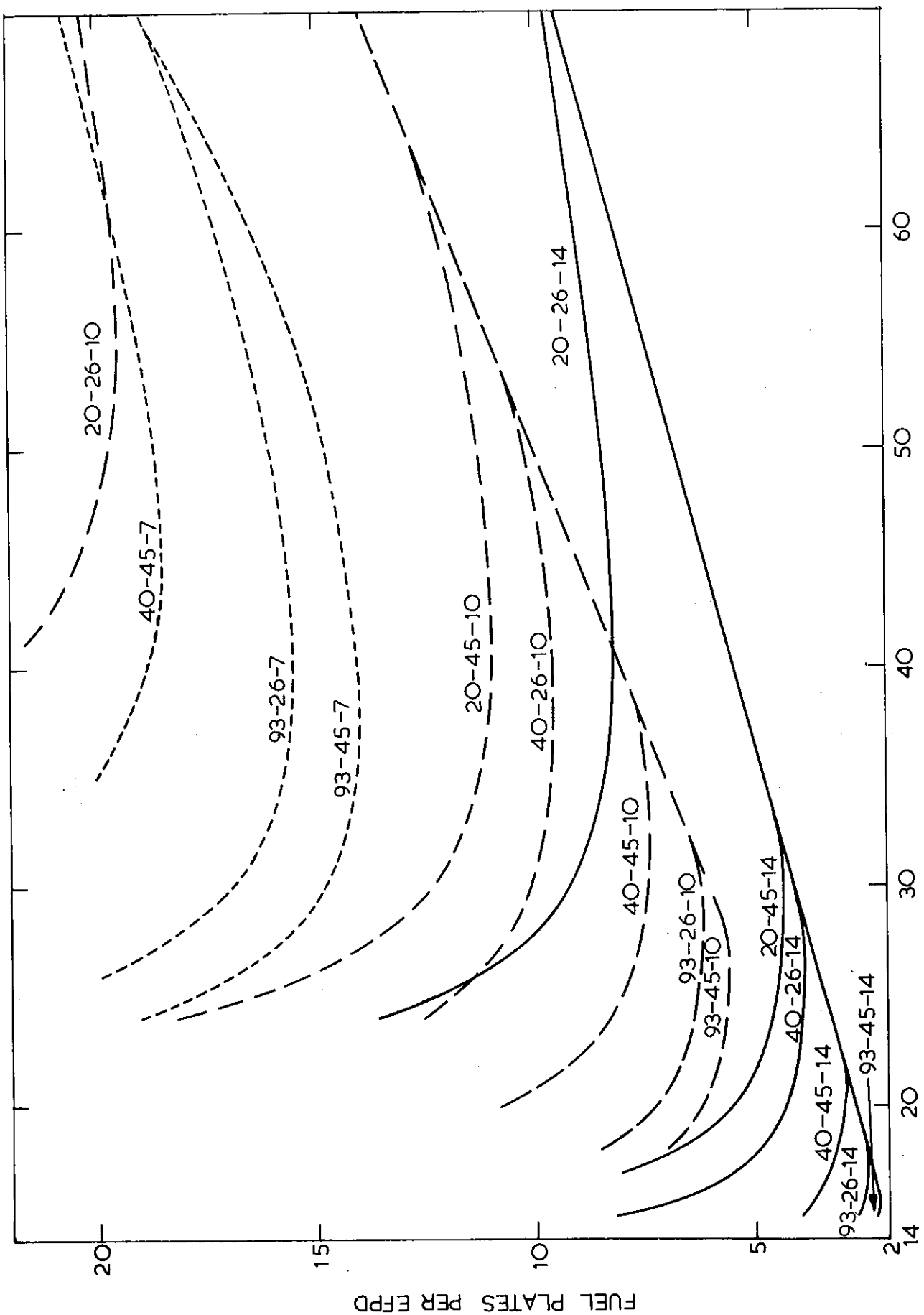

FIGURE 7. FUEL CONSUMPTION RATE

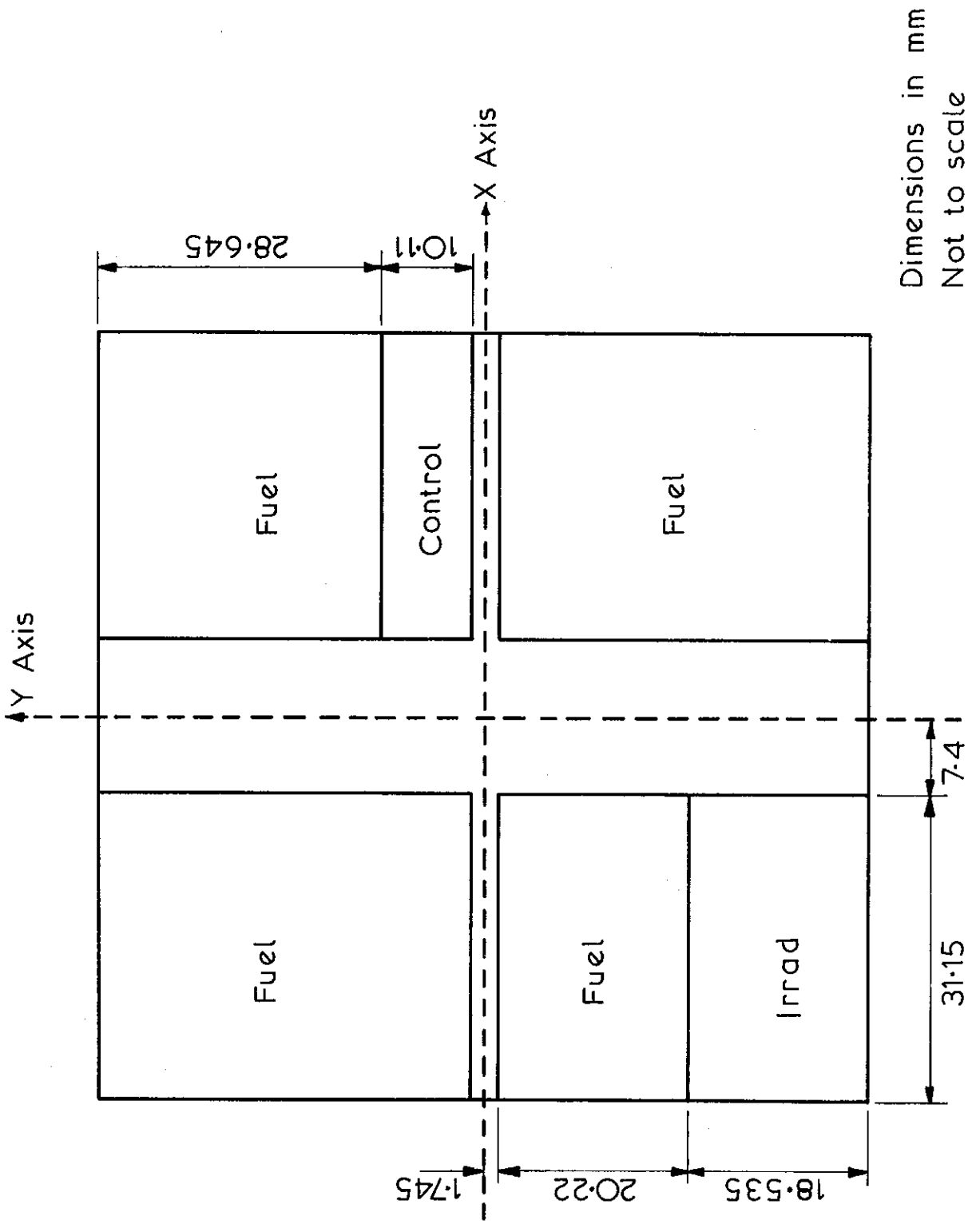

FIGURE 8. SUPERCELL MODEL

APPENDIX A

DETAILS OF THE CALCULATIONS

A.1 MATERIALS

The material densities and compositions used in the calculations are detailed below. Densities are given as atoms per barn cm.

Aluminium	Al	0.0602
Water	H_2O	0.03327
Heavy water	D_2O	0.03314, H_2O 0.0001
Beryllium	Be	0.1235
Irradiation sample	O	0.0189, ZZ999 0.0167, XX999 0.095

The molybdenum trioxide sample was mocked up as ZZ999 a 1/v absorber with a 2200 m s^{-1} cross section of 1 barn, and XX999, which has a resonance integral of 1 barn, because molybdenum data were not available.

The density of the fuel alloy was calculated from the formula

$$\text{density} = 2.85/(1.1666 - \text{uranium weight fraction}),\ \text{g cm}^{-3}.$$

For example, this gives for the 93 per cent enriched, 26 wt % alloy

$$\text{Fuel meat}\ \ ^{235}U - 0.0019478,\ ^{238}U - 0.0001448,\ Al - 0.05193.$$

A.2 FUEL ELEMENTS

The material volume fractions in the core were based on SILOE fuel elements. The standard SILOE fuel element has twenty-three fuel plates of meat dimensions 609.5 x 62.3 x 0.51 mm, which are clad in 0.38 mm Al, except for the outer plates for which the outer cladding is an extra 1 mm thick. (All following dimensions are given as areas extending over the active core height.) The two Al side plates have dimensions 80 x 4.709 mm giving outer fuel element dimensions of 80 x 76.1. The fuel elements are positioned on an 81 x 77.1 pitch. In the model used, the standard fuel element consisted of a fuelled slab region containing fuel meat, normal cladding and water gap occupying a volume fraction of 0.77323. This fuelled region was that used in the slab cell calculation for cross section preparation. Additional aluminium included the two side plates, extra cladding of dimension 66.682 x 2, and the unfuelled portion of the plates which had dimensions 4.382 x 77.51 x t/(t+g), where t and g are the plate and water gap thicknesses, respectively.

A SILOE control element has seventeen fuel plates and four inert plates defining two control blade channels. In the model used, fuel occupied 17/23 of the region occupied in the standard element and the

remaining 6/23 had an aluminium volume fraction of 0.6667t/(t+g).

A SILOE irradiation element has twelve fuel plates and an aluminium block pierced by two vertical holes. In the model used, fuel occupied 12/23 of that for the standard element and the remaining 11/23 was aluminium, except for a sample area of 200 π and a water area of 150 π. This represents two 20 mm diameter MoO_3 samples and some water in the holes.

Using fuel element numbers for standard, control and irradiation elements in the ratio 21:5:6, the core volume fractions are:

Fuelled slabs	0.67237
Extra aluminium	0.17834 + 0.0754t/(t+g)
Extra water	0.13043 - 0.0754t/(t+g)
Sample	0.01886

The resulting overall water fraction is 0.8028 - 0.7478t/(t+g). Additional information is given below.

A.3 SUPERCELL MODEL

To represent the flux peaking within the various fuel element types, a supercell model was adopted. The model consisted of four 1/4 fuel elements, as shown in Figure 8, with reflective boundary conditions on all outer boundaries. The model included two standard elements, a control element and an irradiation element. The material volume fractions in each zone on the figure are given by:

Fuel - active zone of fuel meat, clad, water gap;

Control - Al 0.6667t/(t+g), H_2O 1 - 0.6667t/(t+g);

Irradiation - Al 0.52389, H_2O 0.20405, Sample 0.27206;

Remainder - Al 0.62617 + 0.23983t/(t+g), H_2O 0.37383 - 0.23983t/(t+g).

This model was used only to calculate fluxes for smearing within each element type. Simple volume smearing was used to form average core cross sections.

A.4. GENERATION OF CORE CROSS SECTIONS

The generation of cross sections for materials in the core as a function of burnup was performed in a cell burnup calculation. The cell consisted of three infinite length slabs of half the fuel meat thickness, 0.38 mm of cladding and half the water gap. The function performed by each AUS module is described in turn.

The MIRANDA module [Robinson 1977] is a data preparation code based on multiregion resonance theory which employs a 128-group cross section

library derived from ENDFB/IV. The resonance treatment is a subgroup method which uses collision probability routines to represent spatial effects. Condensation to fewer groups is also performed following a homogeneous B_n spectrum calculation. The code was used to perform a three-region resonance calculation (fuel, Al, H_2O), a B_1 flux calculation, and condensation of the cell materials and nuclides to 26 groups. The B_1 calculation included a buckling search to give a k_{eff} of 1.08.

The ICPP module is based on collision probability routines [Doherty 1969] which make the assumption of a flat group-source in each mesh interval. This module was used to perform a 26-group k_∞ calculation with the cross sections prepared in MIRANDA. The mesh intervals used were two equal intervals in the fuel meat, one in the clad and four equal intervals in the water.

The EDIT module [J.P. Pollard, AAEC unpublished report] was used to edit the flux output of ICPP to form cell average cross sections, to perform a homogeneous flux calculation which included a buckling to give $k_{eff} = 1.08$, and to condense to five-group cross sections. Cross sections were generated for the slab cell, Al, H_2O, the irradiation sample and a 1/v absorber.

The CHAR module is a multiregion burnup module [Robinson 1975b] which uses analytic techniques to perform nuclide burnup using spatial fluxes from other AUS modules. The code made use of ICPP fluxes adjusted to criticality by EDIT. The power level used was 144 watts per cm^2 of active plate area. Because the analytic method requires constant flux level, the major time step of 0.0472 MWd g^{-1} was divided into six intervals with power normalisation at the beginning of each step.

After each major time step, which was the time step needed to give a burnup of 0.0472 MWd/g of ^{235}U, the calculation sequence was repeated from the MIRANDA step.

The supercell calculation was performed in five groups using the POW diffusion module [Pollard 1974]. POW is a two-dimensional diffusion code which uses edge mesh points. The calculation was performed for a burnup of 0.236 MWd g^{-1} only and the same fluxes used for other burnups. The mesh intervals used in the calculation were:

X direction - three of 10.38333, two of 7.4, three of 10.38333,

Y direction - four of 4.63375, four of 5.055, two of 1.745, four of 5.055, four of 4.63375.

A.5 GENERATION OF REFLECTOR CROSS SECTIONS

Reflector cross sections were prepared in the MIRANDA module by condensing to five groups over homogeneous calculations with a ^{235}U fission spectrum source. The spectrum defining material was H_2O for H_2O and Al cross sections, heavy water for heavy water cross sections and a mixture of 90 per cent Be, 10 per cent H_2O for Be cross sections.

A.6 REACTOR CALCULATIONS

Reactor calculations were performed with the POW module. The quoted fluxes were normalised to a total fission energy rate equal to the quoted power level using an energy release per fission of 3.2×10^{11} J or 199.75 MeV. This energy/fission includes some allowance for gamma heating. In those calculations (Sections 3.2, 3.3 and 3.4) in which the calculation was not adjusted to criticality, the fluxes were normalised to k_{eff} times the power level so that thermal fluxes in the core were slightly in error. Though POW is an edge mesh code, fluxes and form factors are quoted for mesh intervals rather than for mesh points.

In all RZ calculations, the Z mesh intervals (in mm) used were nine of 30.475, five of 6.095, five of 6, four of 30 and three of 50, the last two being in the surrounding water. The R mesh intervals in the core were nine of 0.1 of the core radius and four of 0.025 of the core radius. For D_2O reflectors the reflector mesh was one of 12 in the Al, eight of 25 and fourteen of 50, the last two being in water. Additional mesh intervals were assigned to water as the D_2O width was reduced. For 400 mm wide Be reflectors, the reflector mesh used was ten of 20, five of 40, five of 20 and two of 50. For 300 and 200 mm wide Be reflectors, the mesh was twenty of 20 and two of 50.

The following mesh intervals were used in XY calculations. In case 1, both X and Y mesh were nine of 22.353, three of 7.4507, one of 12, six of 25, five of 50, four of 100 and two of 50. In case 2, the X mesh was nine of 22.353, three of 7.4507, five of 20, five of 40 and four of 50, and the Y mesh was two of 50, four of 40, four of 20, three of 7.4507, eighteen of 22.353, three of 7.4507, one of 12, six of 2.5, five of 50, four of 100 and two of 50. Case 3 had a reflector mesh identical to that of case 2, but all core mesh intervals were 18.6267. Cases 4 and 5 also had the same reflector mesh, but the core X mesh was twenty-eight of 19.275 and the core Y mesh was twenty of 20.25. Thus each smeared fuel element in case 5 had four mesh intervals in both directions.